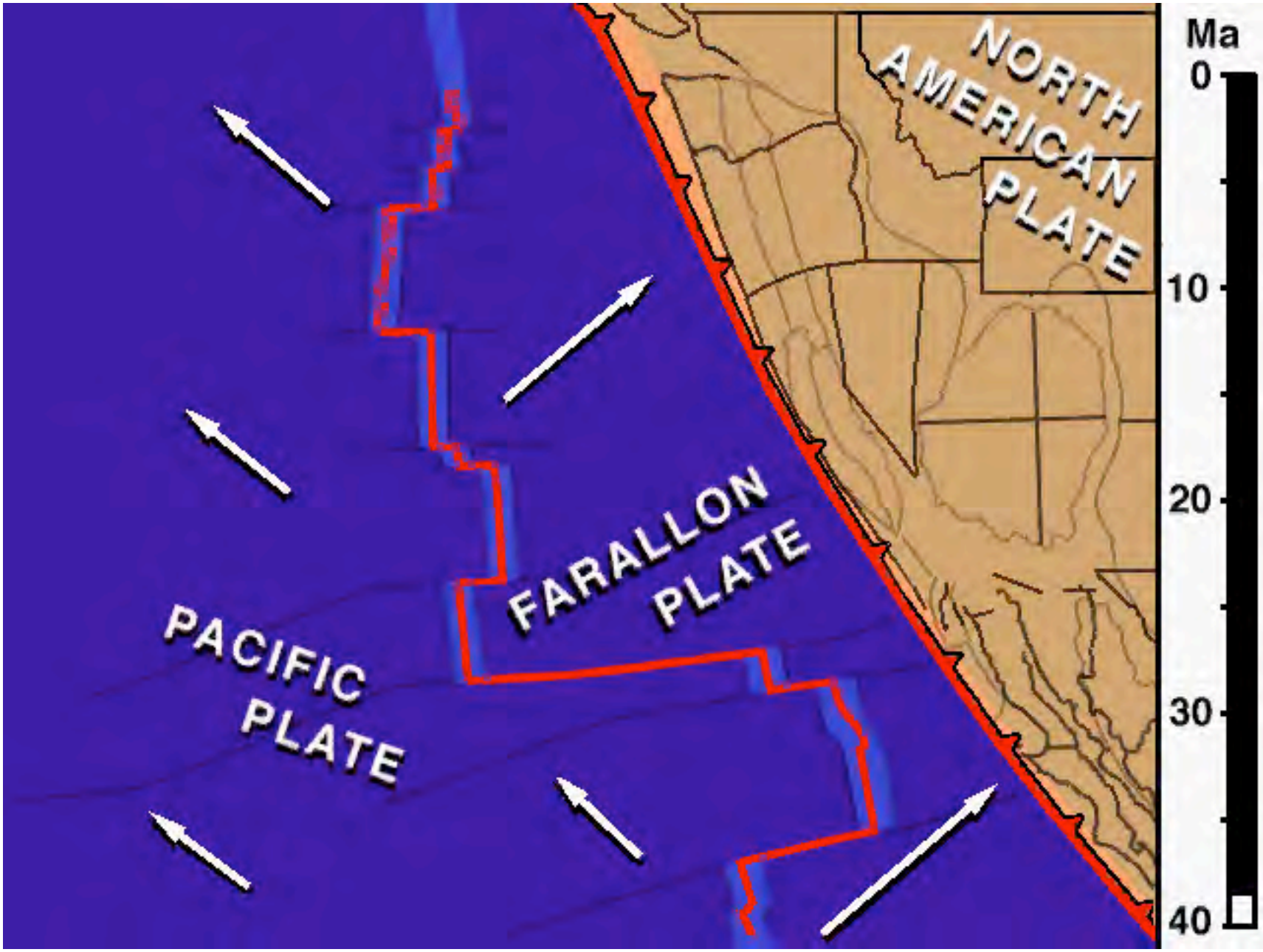
NORTH AMERICAN PLATE
FARALLON PLATE
PACIFIC PLATE
Ma
0
10
20
30
40

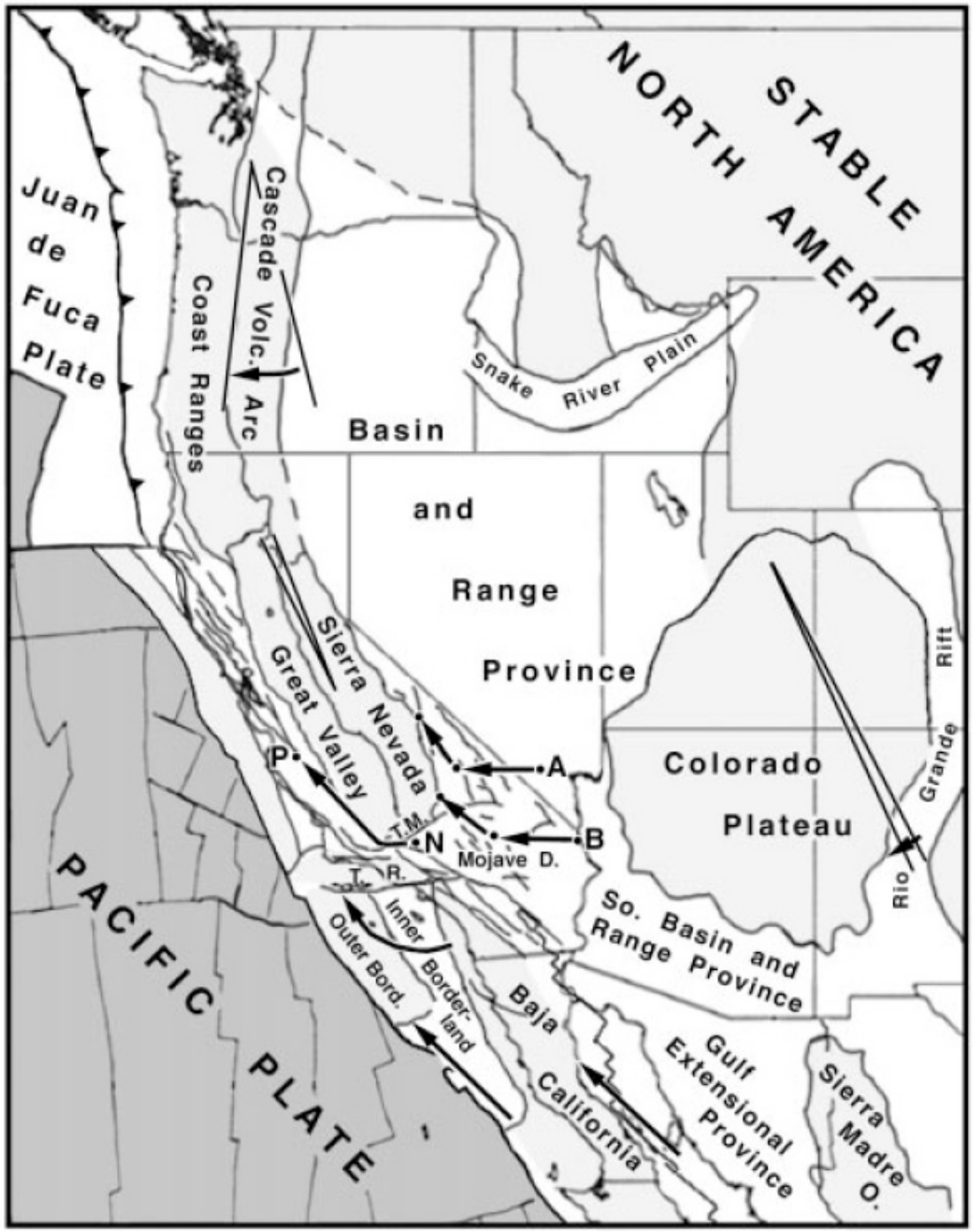

Atwater and Stock 1999

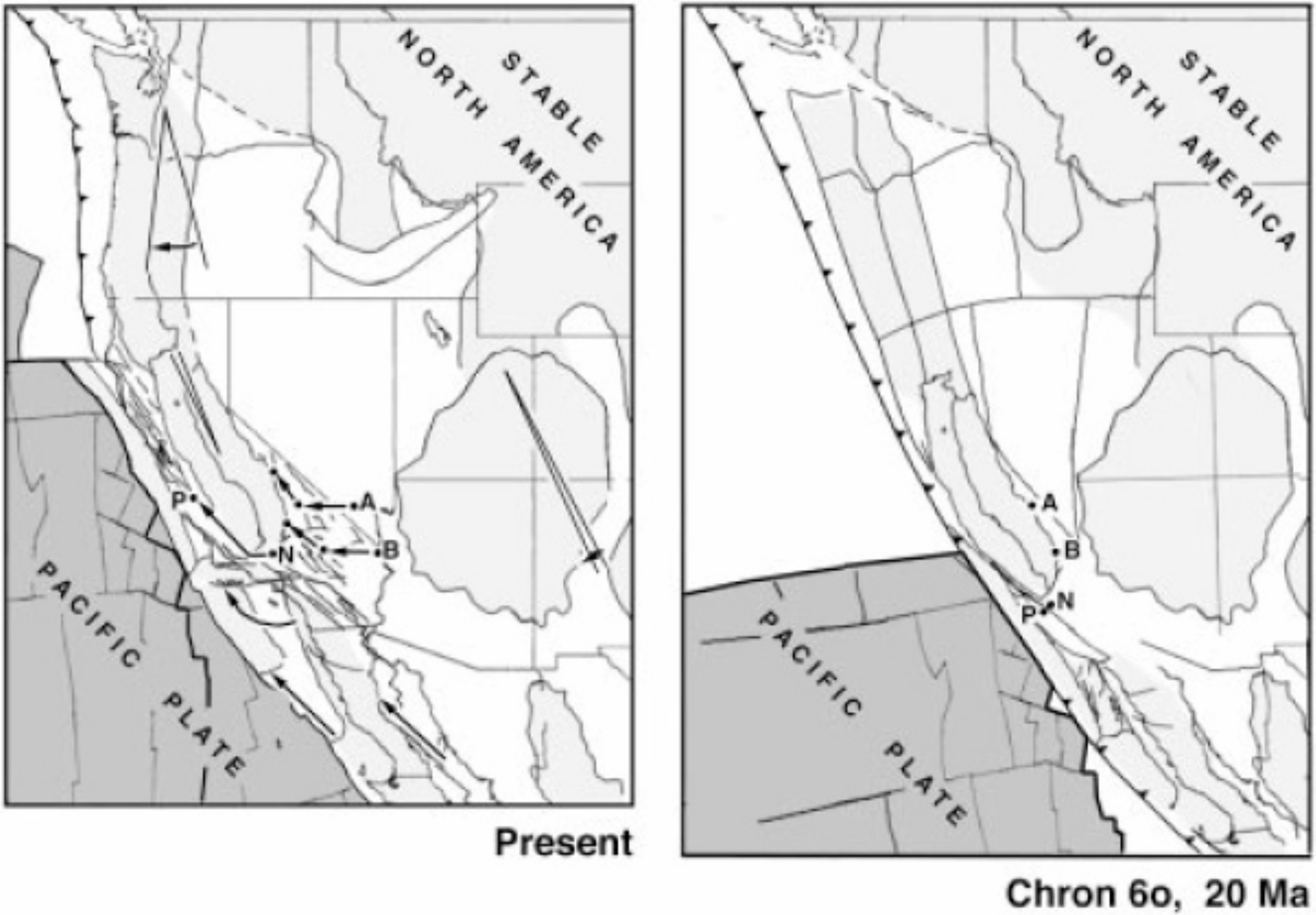

Atwater and Stock 1999

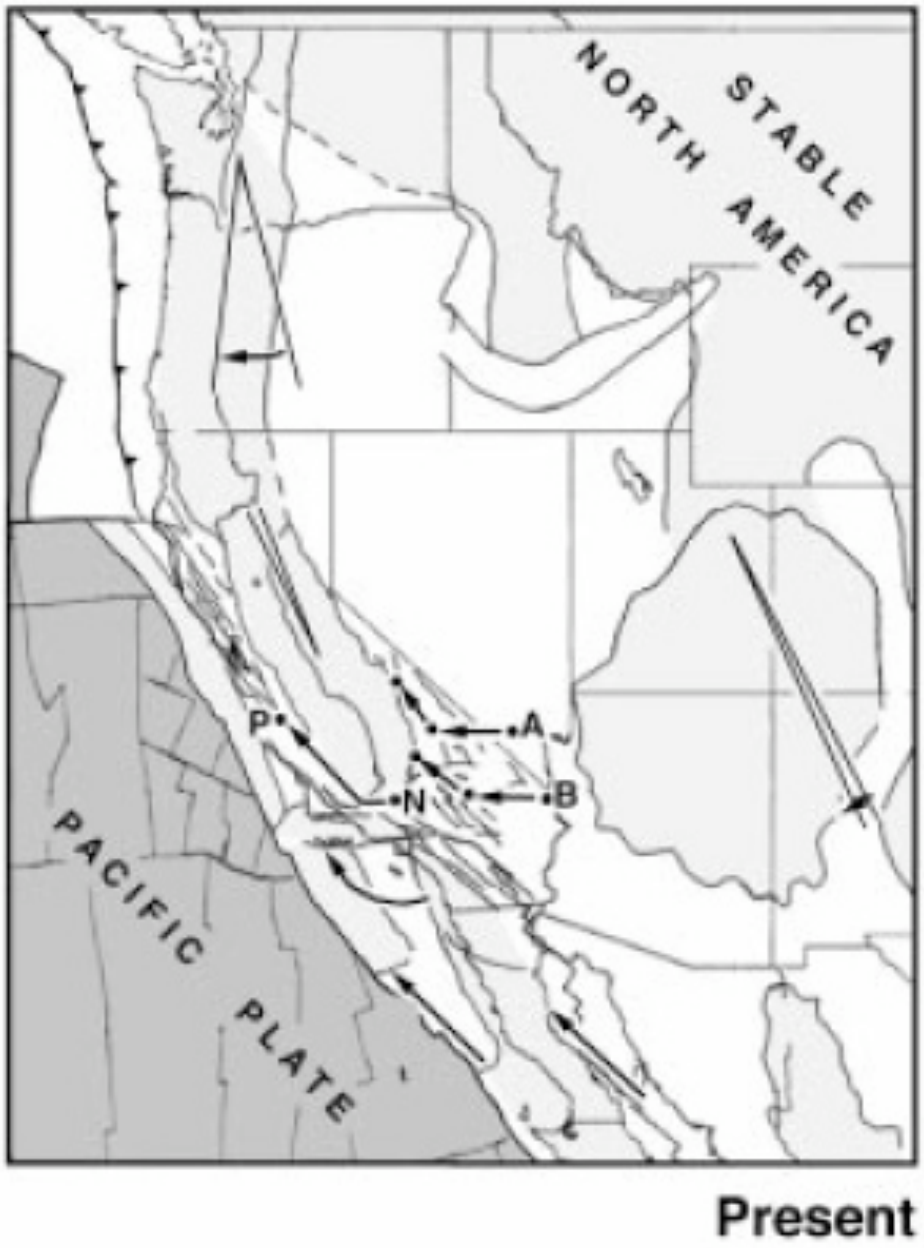

Present

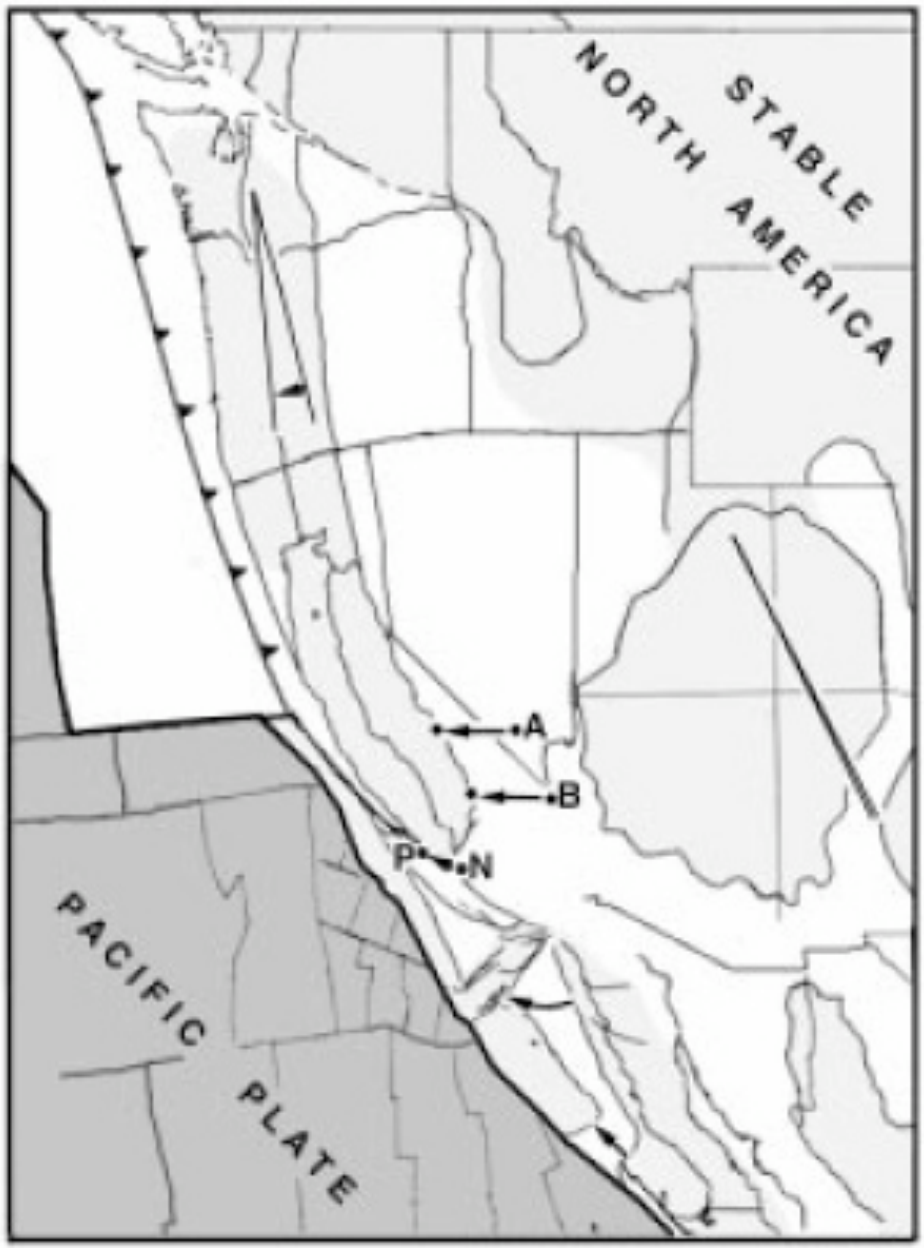

Chron 5o, 11 Ma

Atwater and Stock 1999

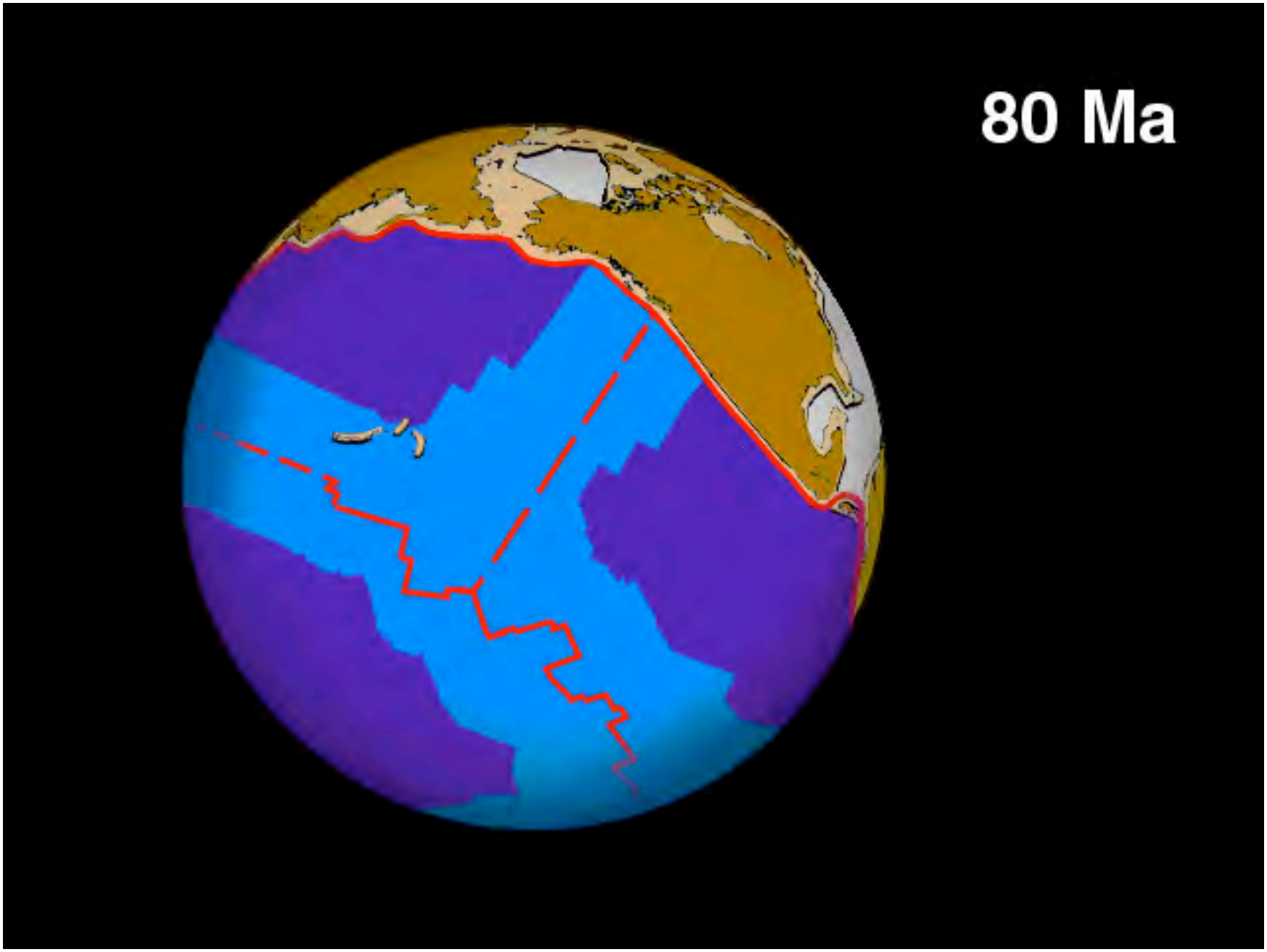
80 Ma

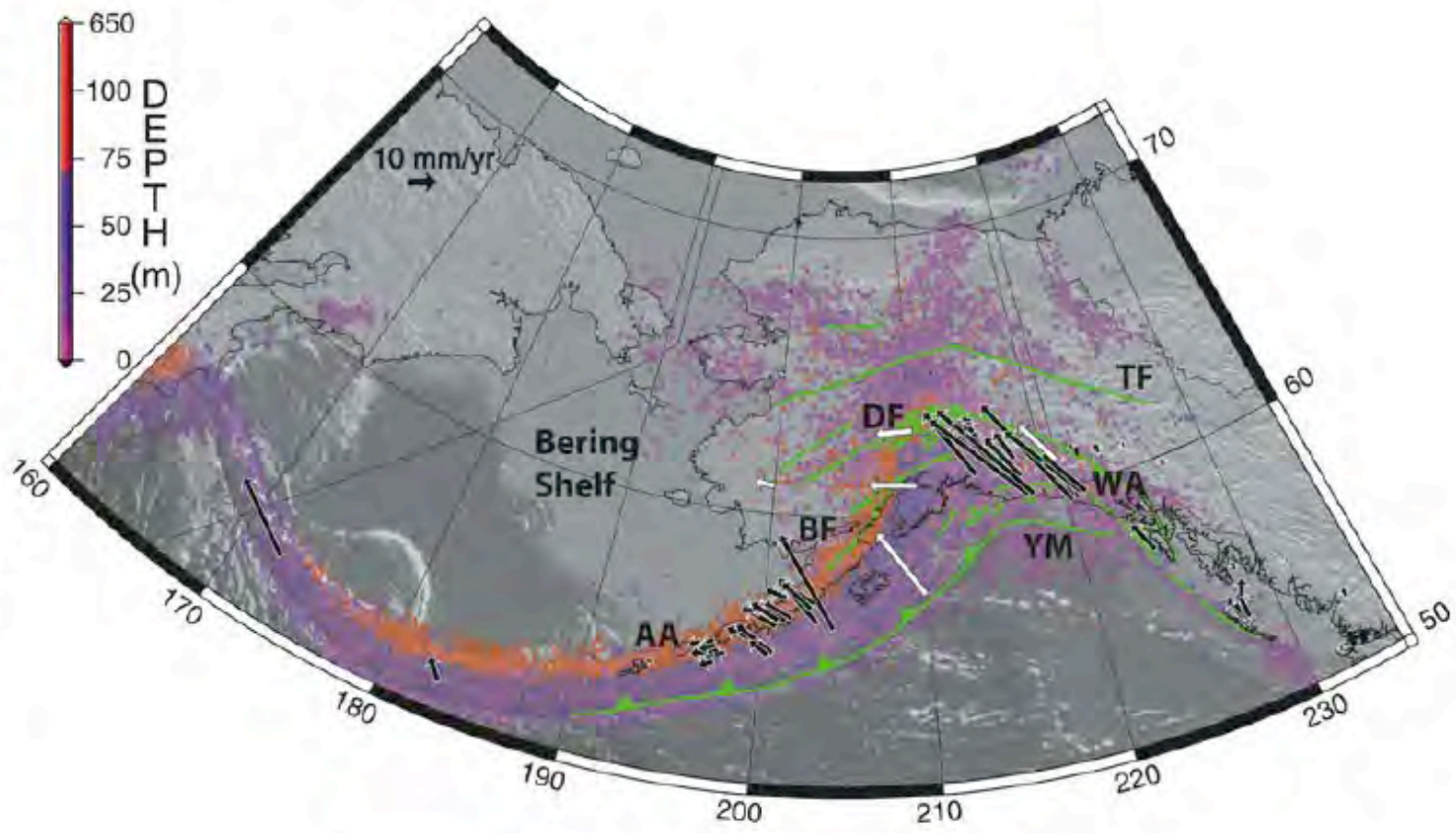

Figure 1. Southern Alaskan convergent margin. Green line segments denote major faults. Colored dots show locations of earthquakes >M_w = 3 from the Alaska Earthquake Information Center. Black vectors represent GPS observations from Sauber et al. (1997), Mazzotti et al. (2003), Fournier and Freymueller (2007), Fletcher and Freymueller (2003), and Avé Lallemant and Oldow (2000); white vectors show kinematic model velocities from Flesch et al. (2007). AA—Aleutian Arc; BF—Bruin Bay fault; TF—Tintina fault; DF—Denali fault; WR—Wrangell Arc; YM—Yakutat microplate.

Kasatochi Volcano (August 7, 2008 eruption), Aleutians

http://alaska.usgs.gov/science/kasatochi/2008_eruption.php

ISS002E6065 2001/05/18 18:00:40

Umniak Island, Aleutians

Mt McKinley (aka Denali) and Mt Foraker, Alaska Range

Anchorage and Chugach Mountains, Alaska

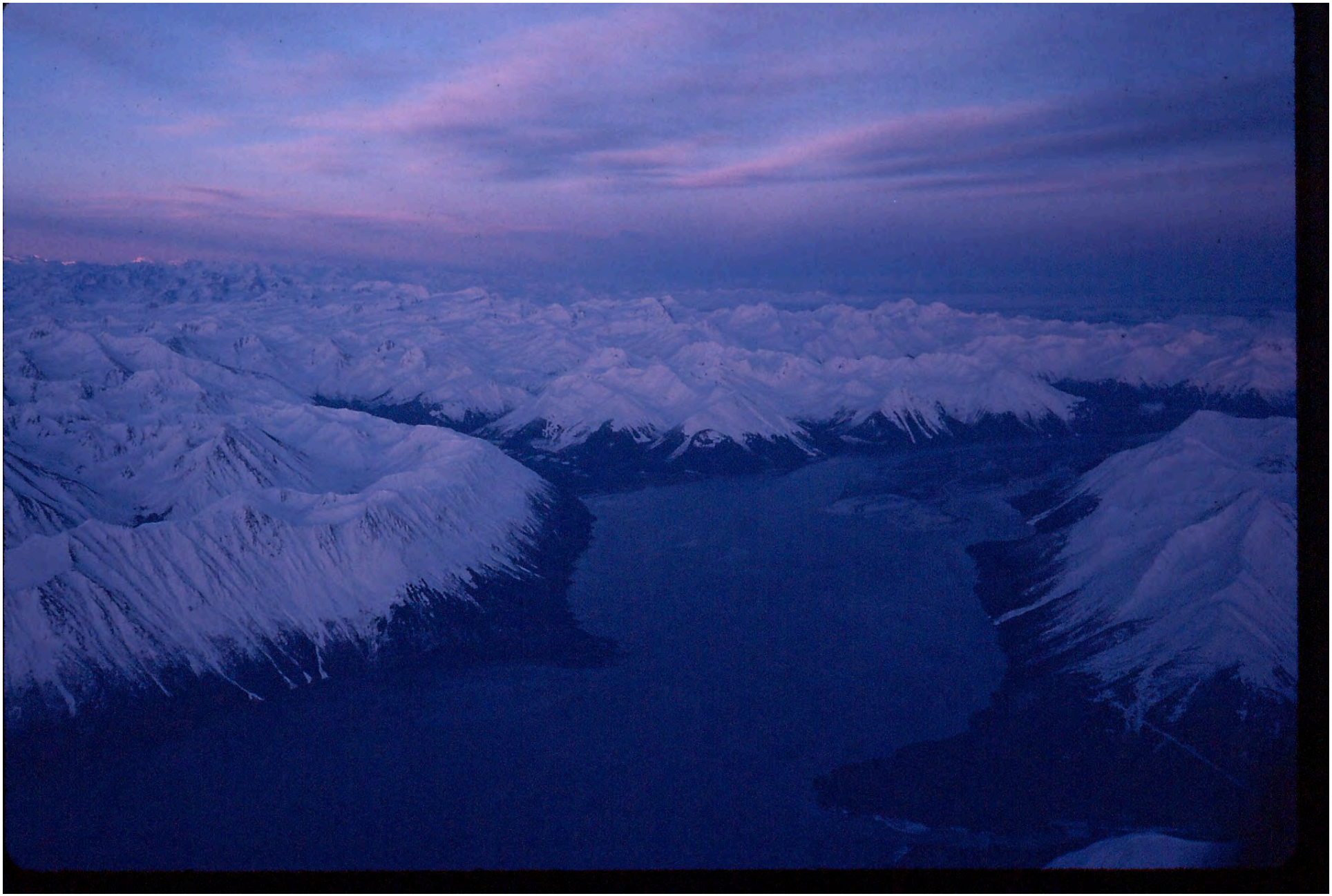

Turnagain Arm and Chugach Mountains, Alaska

Chugach Mountains, Alaska

1 Columbia glacier 2. Valdez Arm 3. Glacier Island 4. Long Bay 5. Chugach Mts

6. Unakwik Inlet 7. Columbia Bay

Malaspina Glacier and Mt St Elias, Alaska and British Columbia


Glacier Bay, Alaska

Strathcombe Park, Vancouver Island, British Columbia

Fraser River delta, Straits of Georgia, British Columbia

Mount Ranier, Mt Adams, Puget Lowlands, Washington

ISS013E54235

Three Sisters, Broken Top, Sparks Lake, Cascade Range, Oregon

Columbia River Basalt Group from Rowena Crest, Oregon

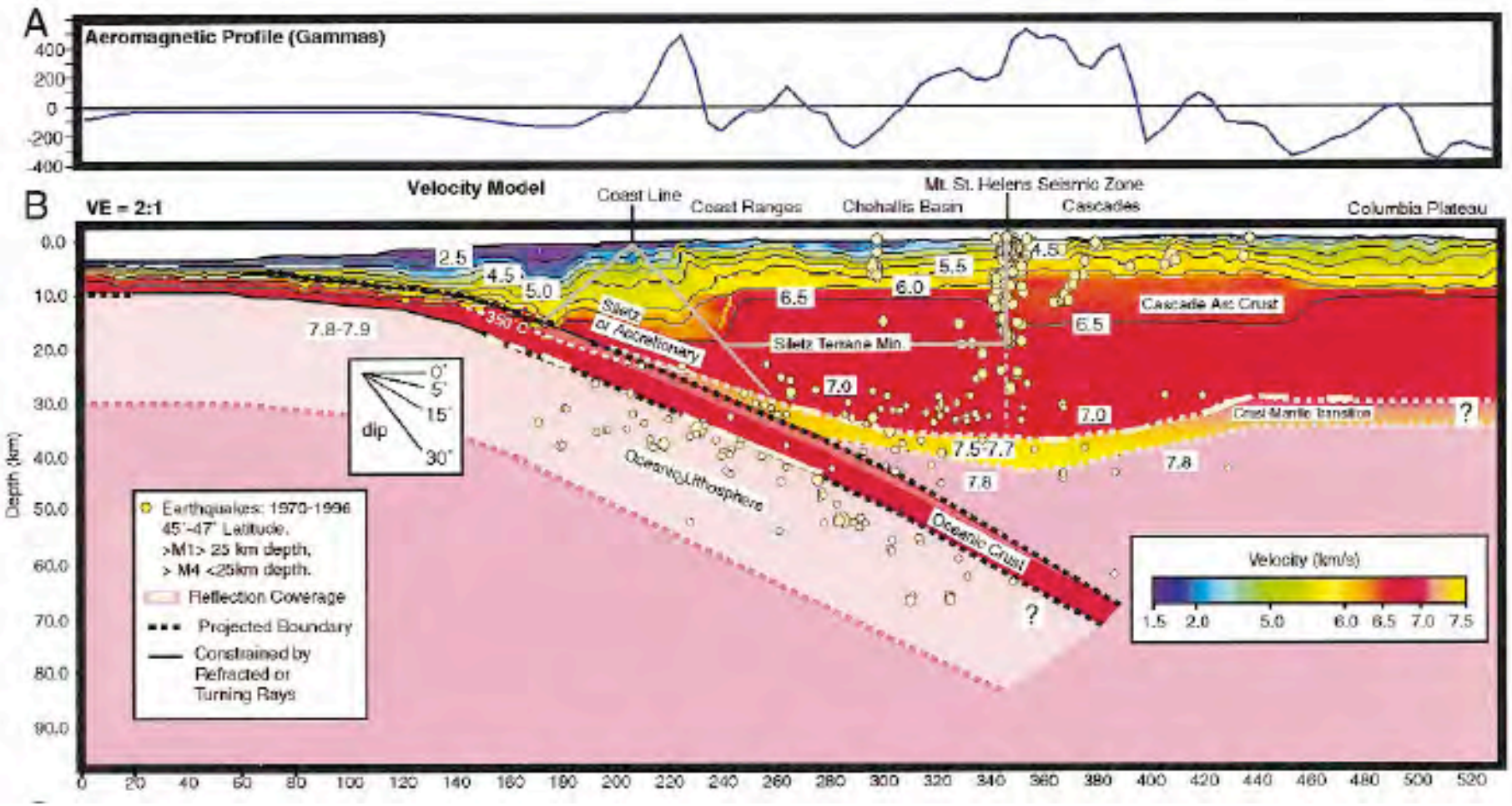

Trehu et al 1996

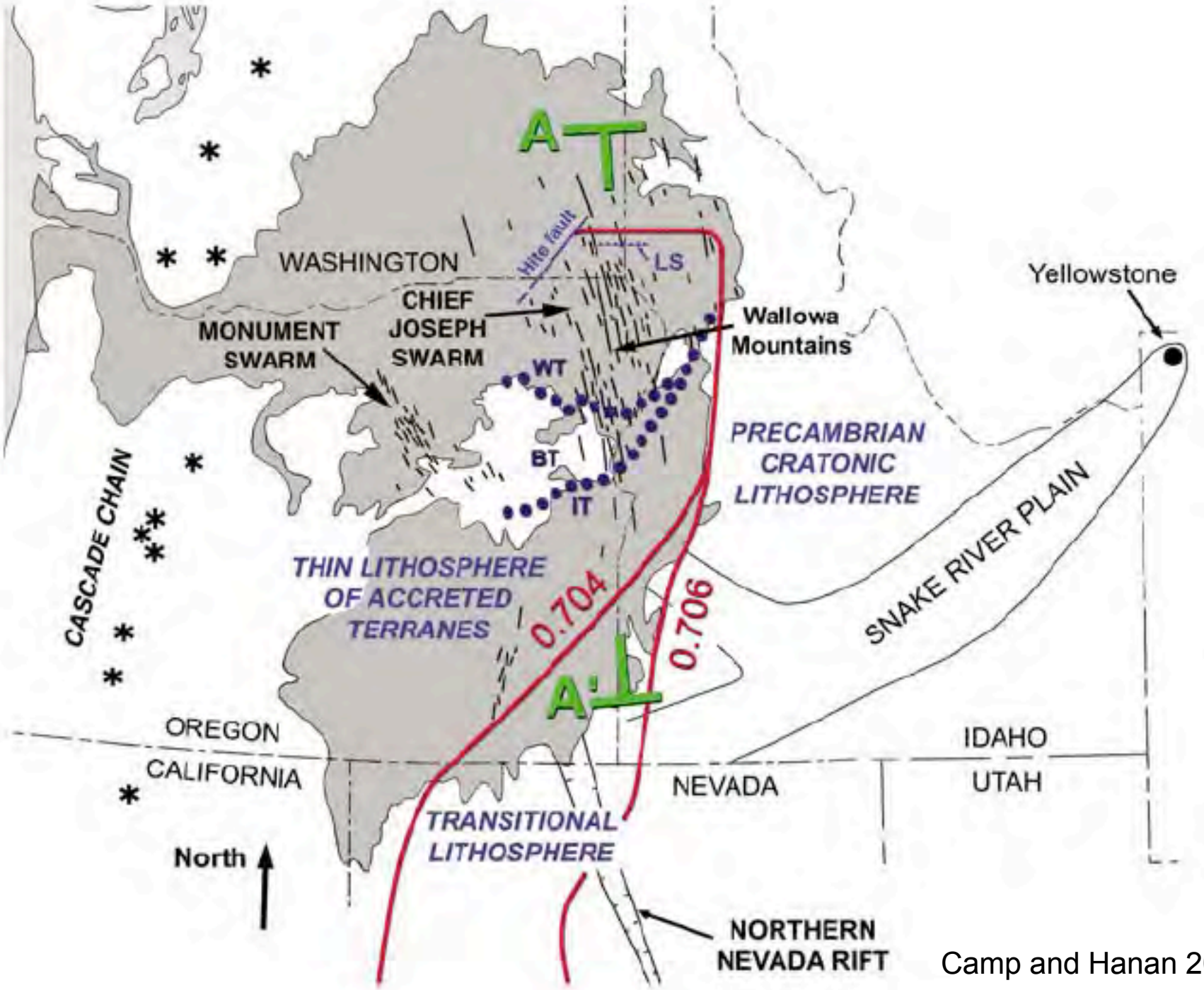

Camp and Hanan 2008

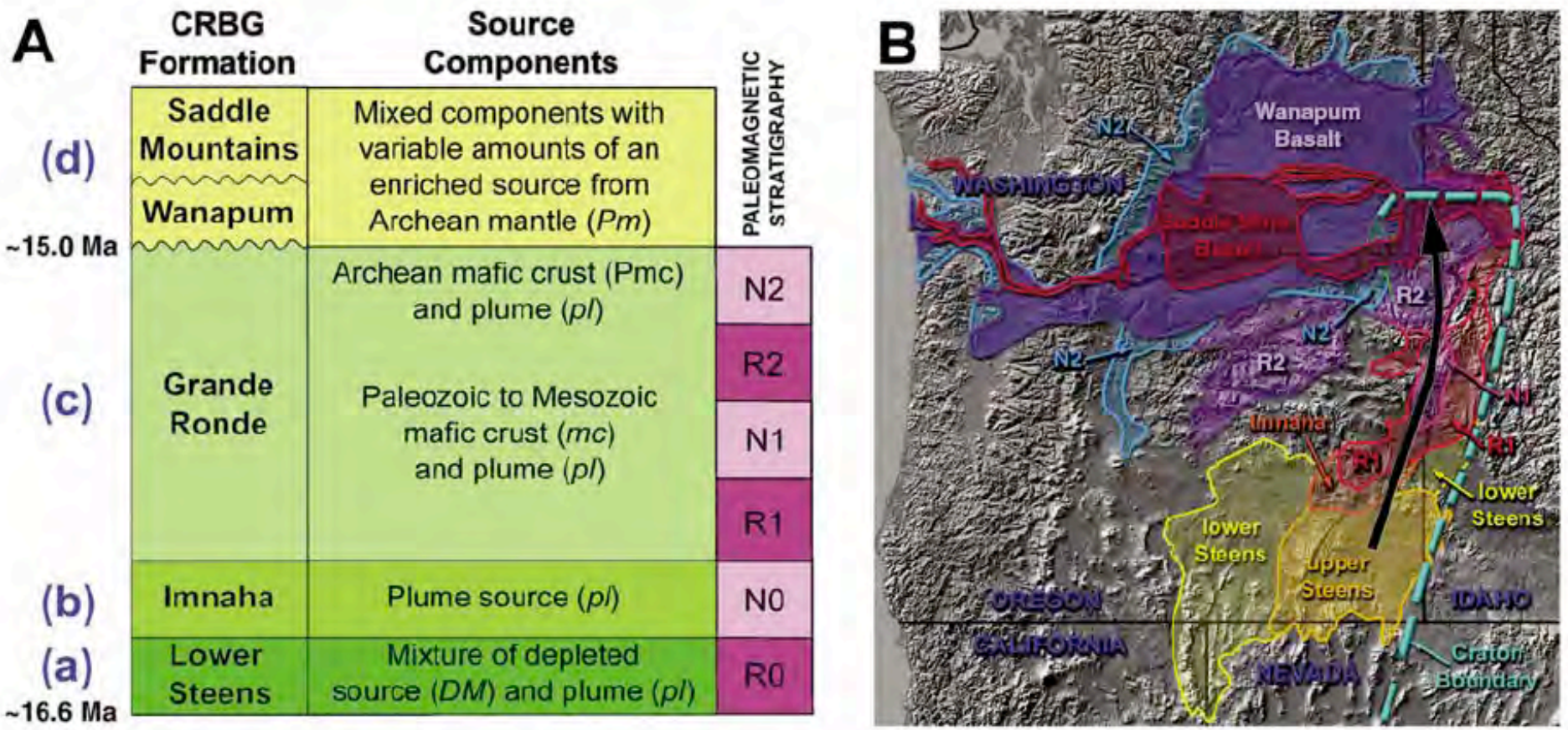

Figure 5. Stratigraphy and map distribution of main Columbia River Basalt Group (CRBG) units. (A) Stratigraphy and

Camp and Hanan 2008

Camp and Hanan 2008

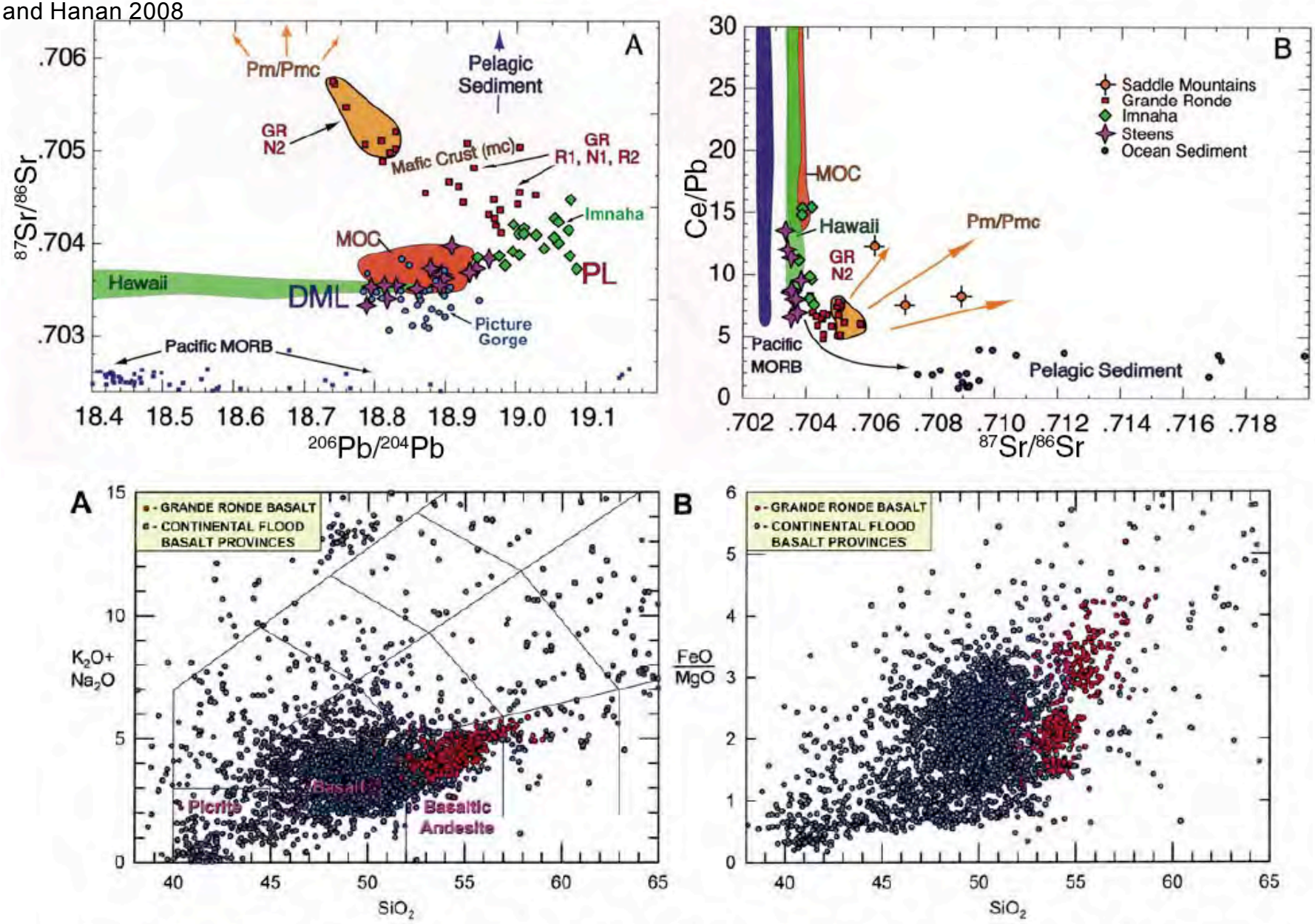

Figure 4. Comparison of 470 analyses of Grande Ronde Basalt with 4466 analyses from well-known continental flood-basalt provinces (Deccan, Ethiopia, Yemen, Parana, Siberia, and Emeishan). (A) Total alkali versus silica diagram (Le Bas et al., 1986). (B) FeO/MgO versus silica diagram. Analyses are from Johnson et al. (1998), Hooper et al. (2002), Camp et al. (2003), and the GeoRoc chemical database (http://georoc.mpch-mainz.gwdg.de/georoc/).

Yakima
Foldbelt

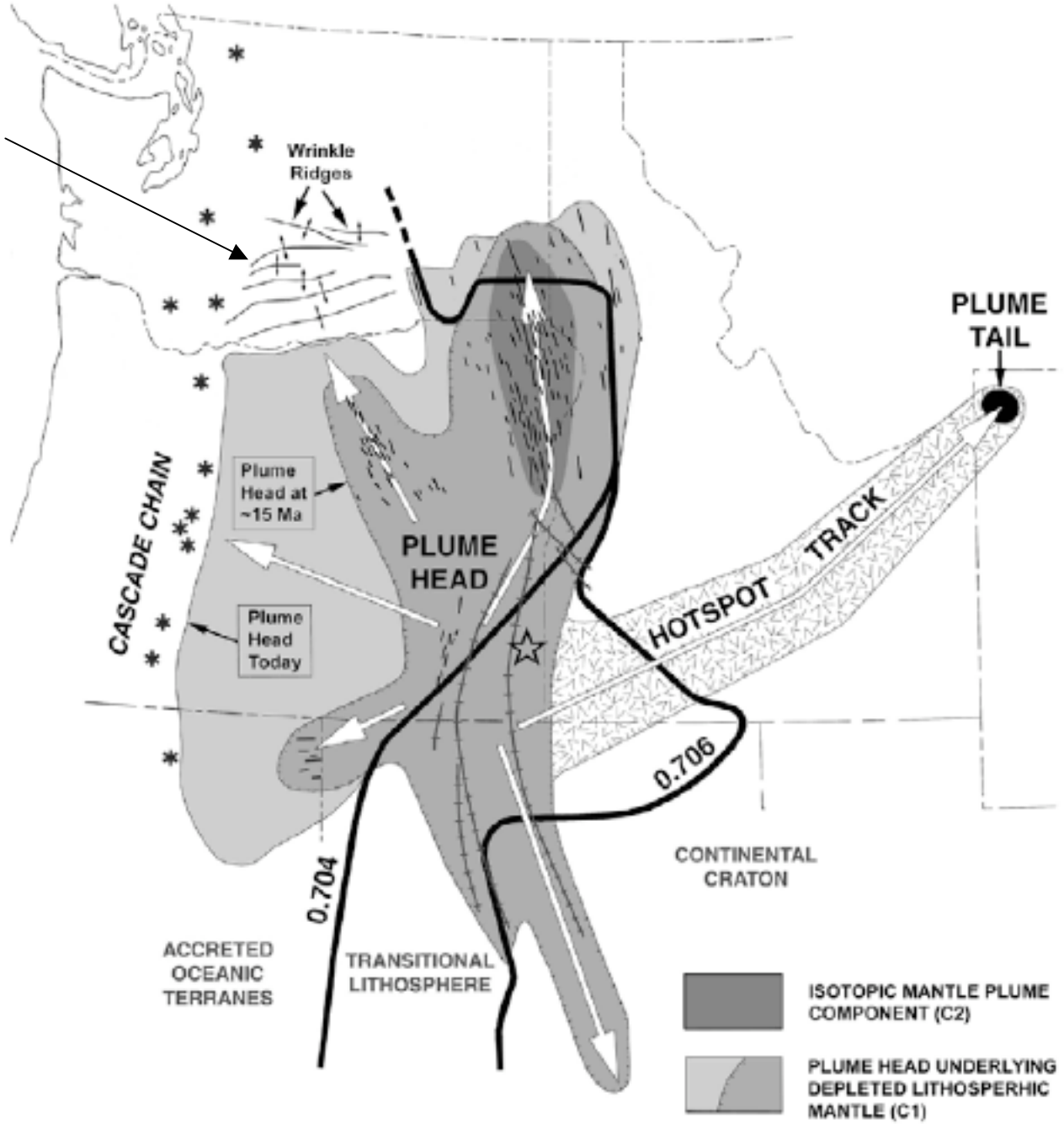

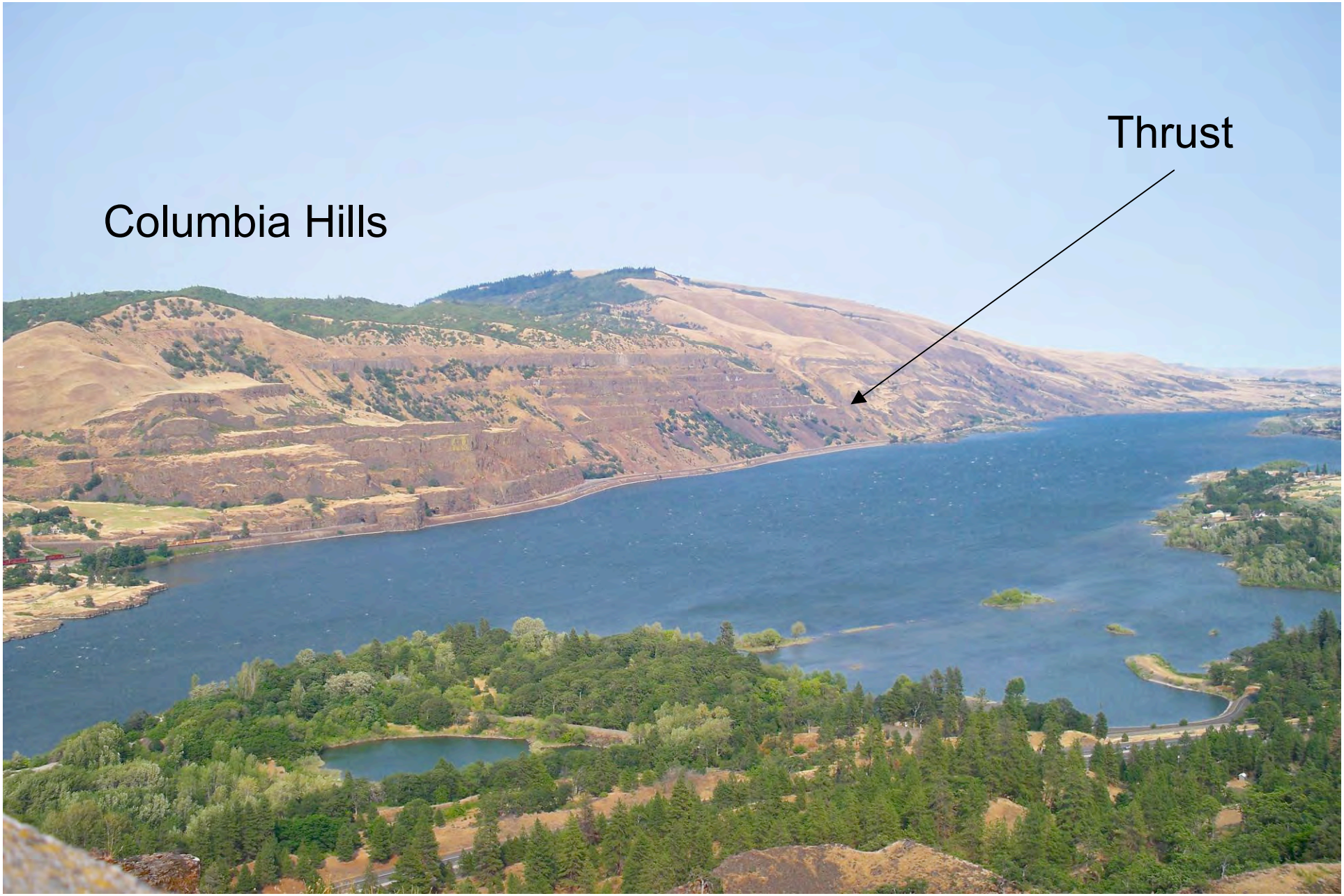

Columbia River Basalt Group from Rowena Crest, Oregon

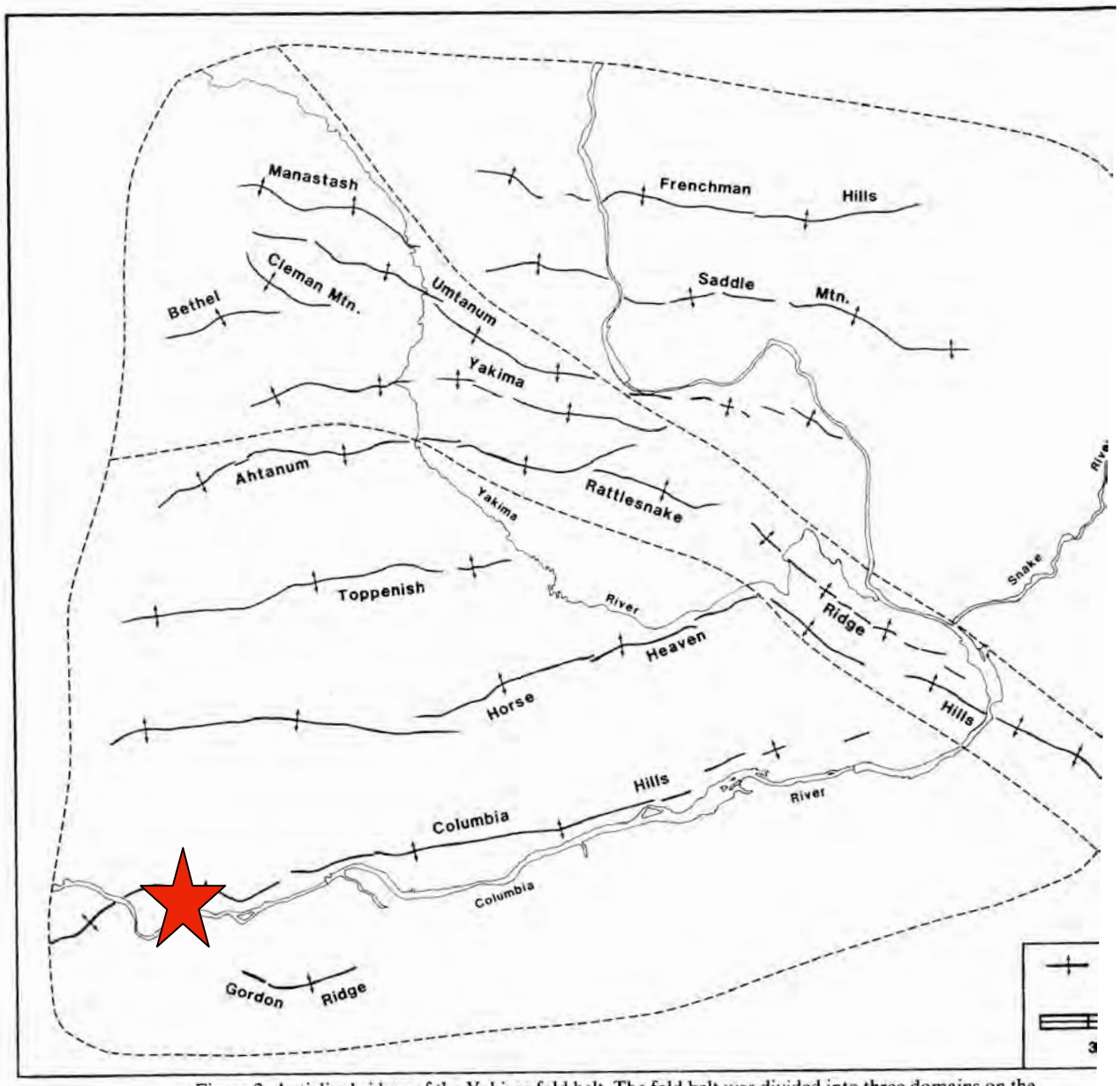

Figure 3. Anticlinal ridges of the Yakima fold belt. The fold belt was divided into three domains on the basis of orientations and spacings of the anticlines. The southern domain contains Gordon Ridge, the Columbia Hills, western segments of the Horse Heaven Hills, Toppenish Ridge, and Ahtanum Ridge. The central domain is made up of eastern segments of the Horse Heaven Hills, Rattlesnake Ridge, Yakima Ridge, western segments of Umtanum Ridge, the Cleman Mountains, Bethel Ridge, and Manastash Ridge. The northern domain contains eastern segments of Umtanum Ridge, the Saddle

Waters 1989

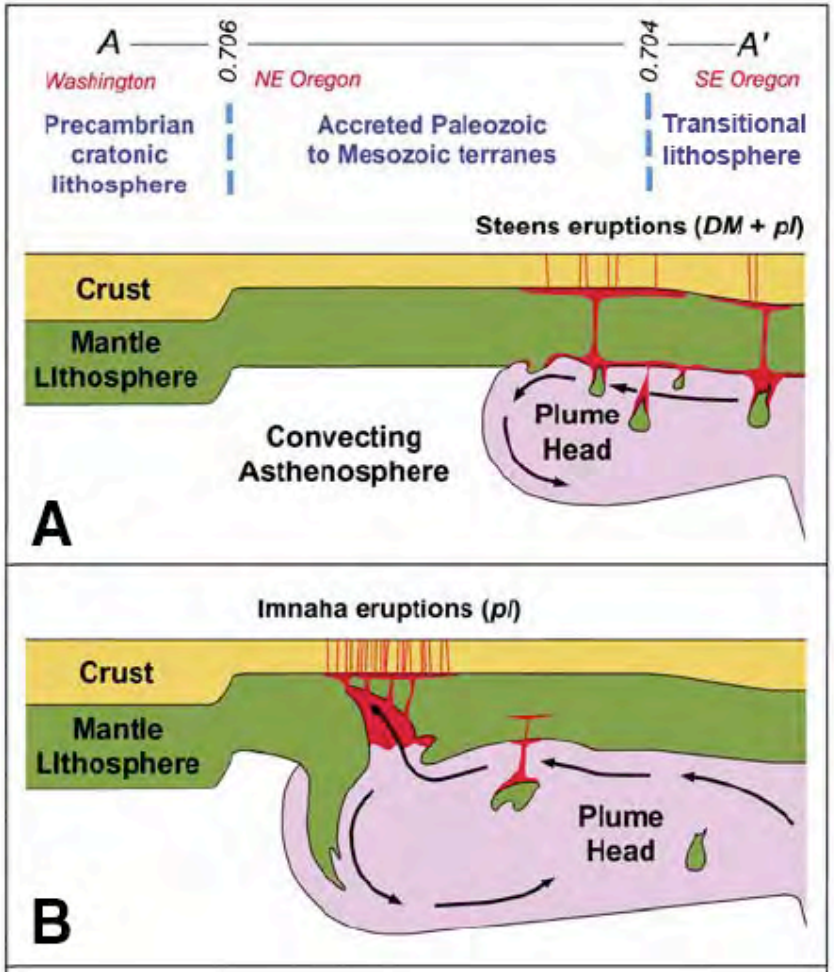

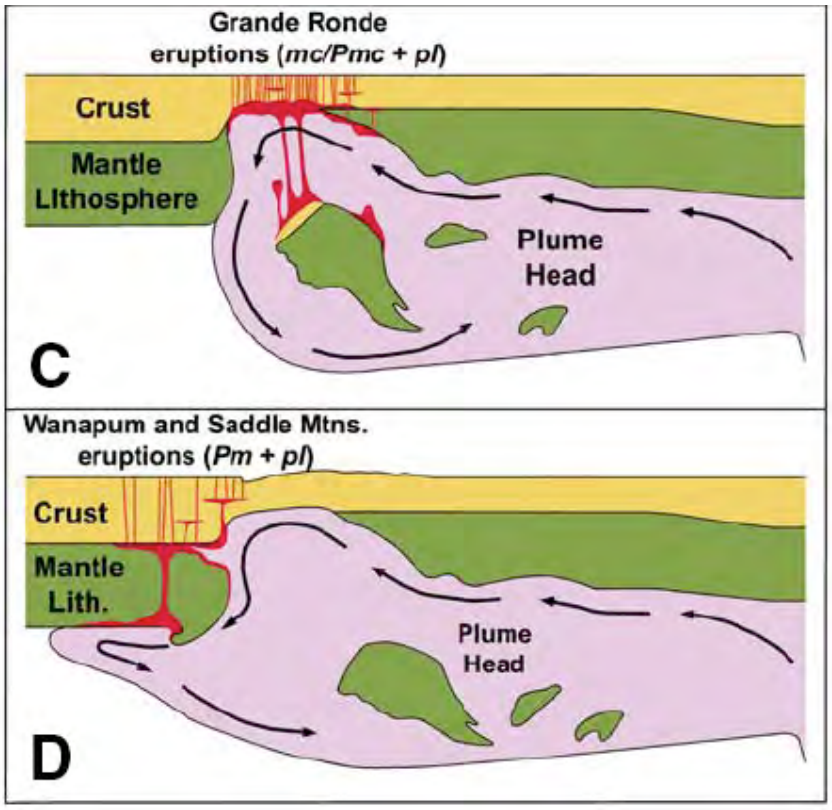

Camp and Hanan 2008

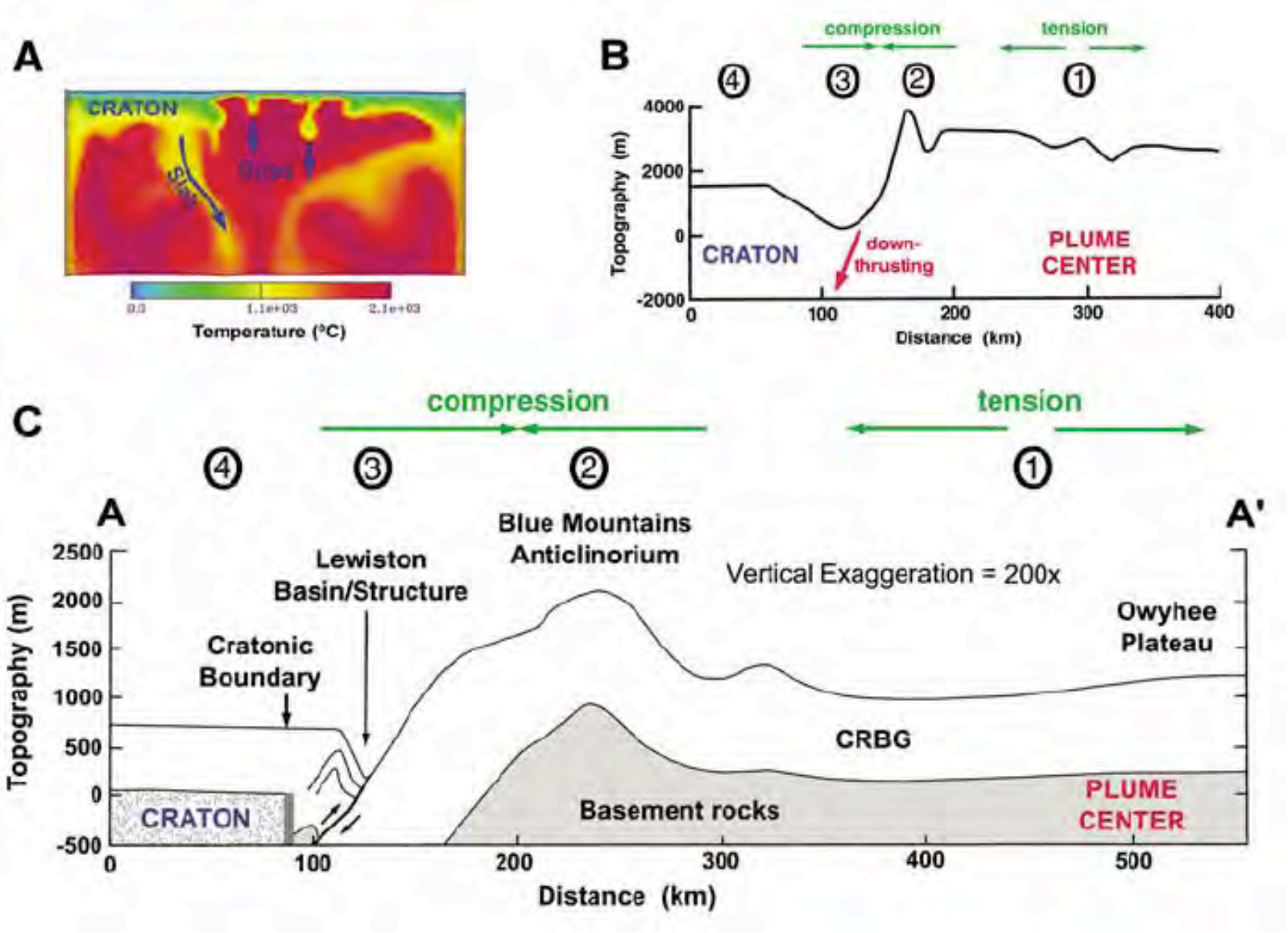

Camp and Hanan 2008

Camp and Hanan 2008

Figure 9. Oblique panoramic view of the Lewiston Basin, with thrust faults and folds of the Lewiston structure marking its northern edge adjacent to the cratonic boundary of North America. To-

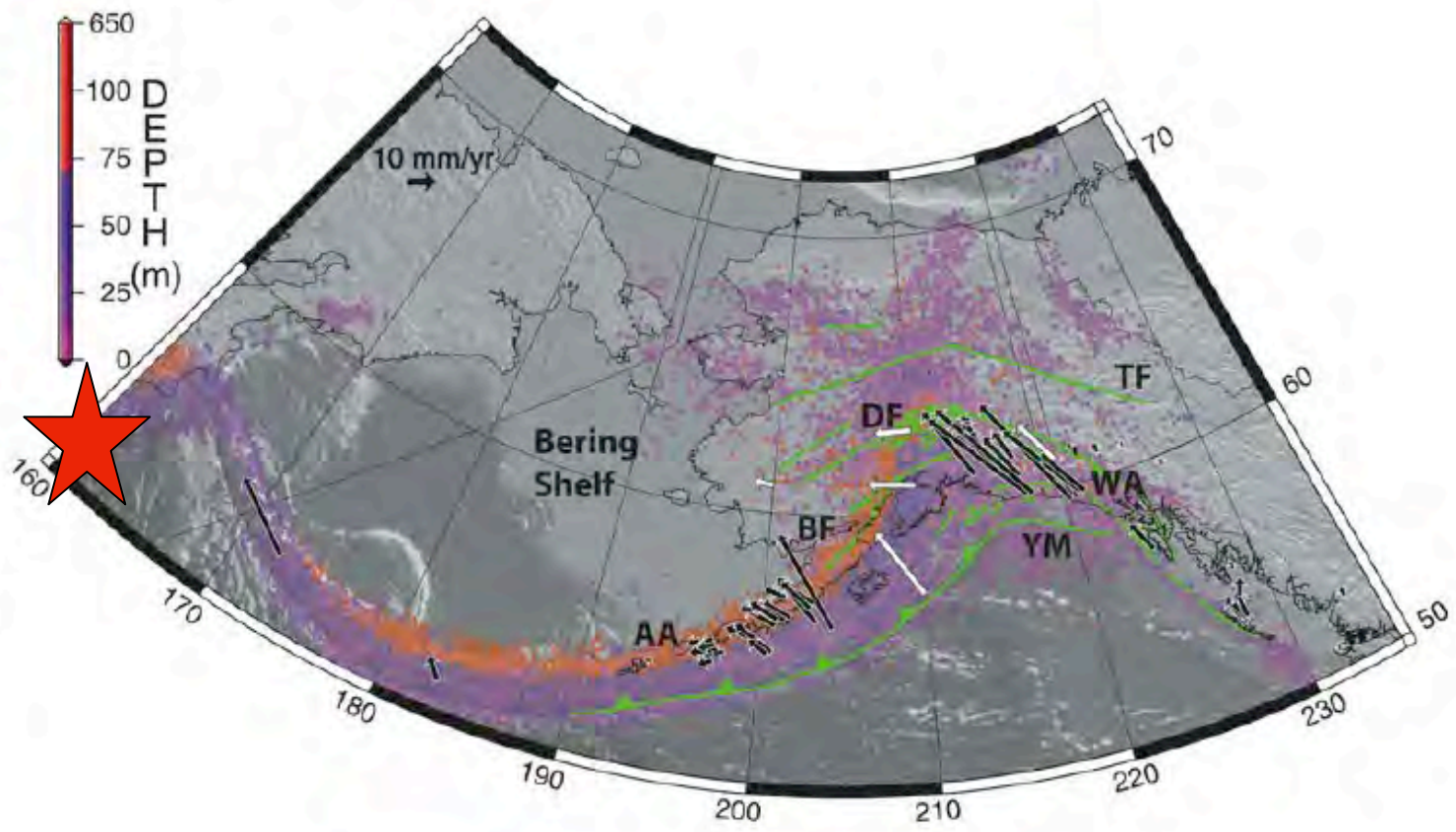

Figure 1. Southern Alaskan convergent margin. Green line segments denote major faults. Colored dots show locations of earthquakes >M_w = 3 from the Alaska Earthquake Information Center. Black vectors represent GPS observations from Sauber et al. (1997), Mazzotti et al. (2003), Fournier and Freymueller (2007), Fletcher and Freymueller (2003), and Avé Lallemant and Oldow (2000); white vectors show kinematic model velocities from Flesch et al. (2007). AA—Aleutian Arc; BF—Bruin Bay fault; TF—Tintina fault; DF—Denali fault; WR—Wrangell Arc; YM—Yakutat microplate.

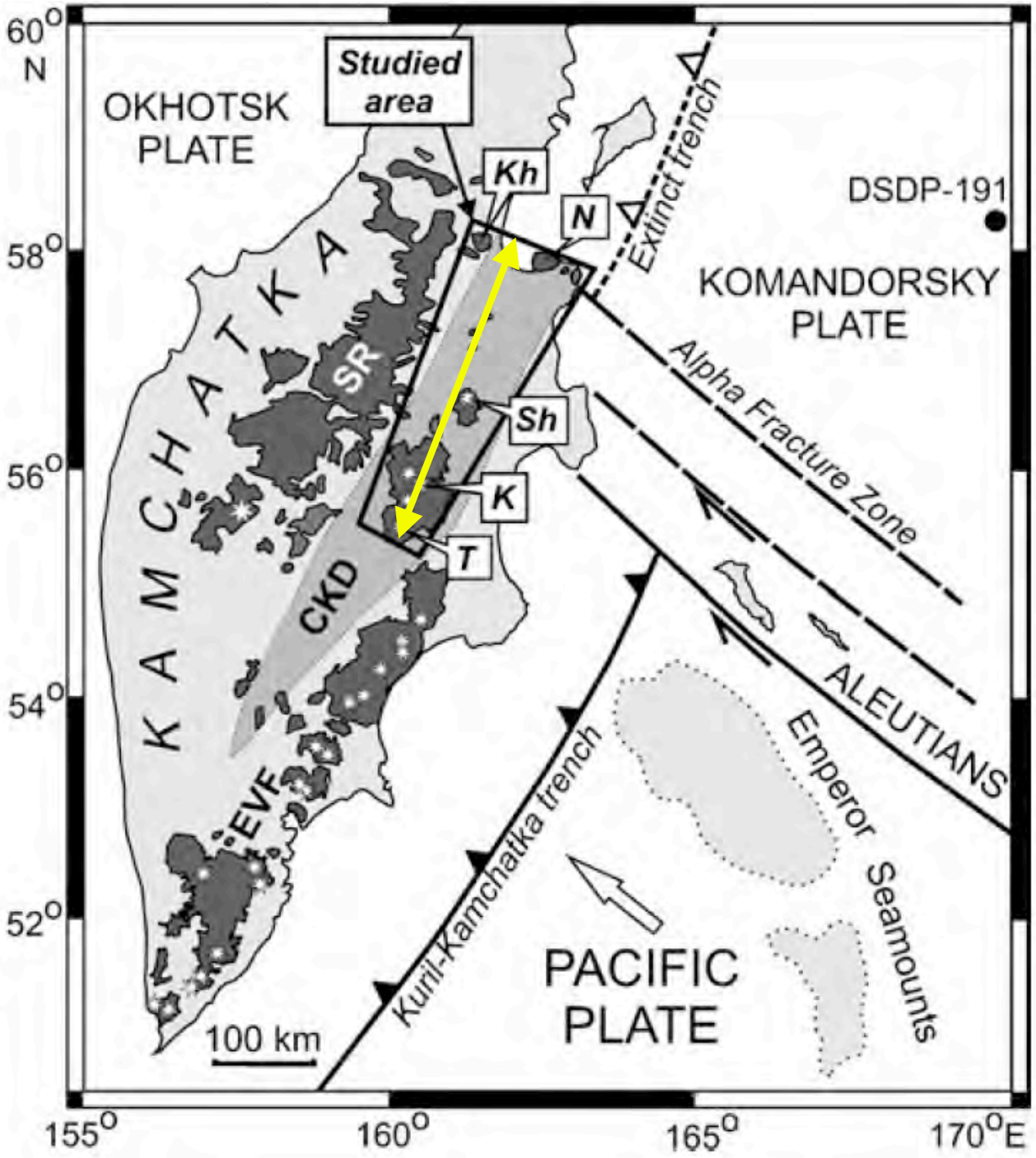

Portnyagin et al 2005

Portnyagin et al 2005

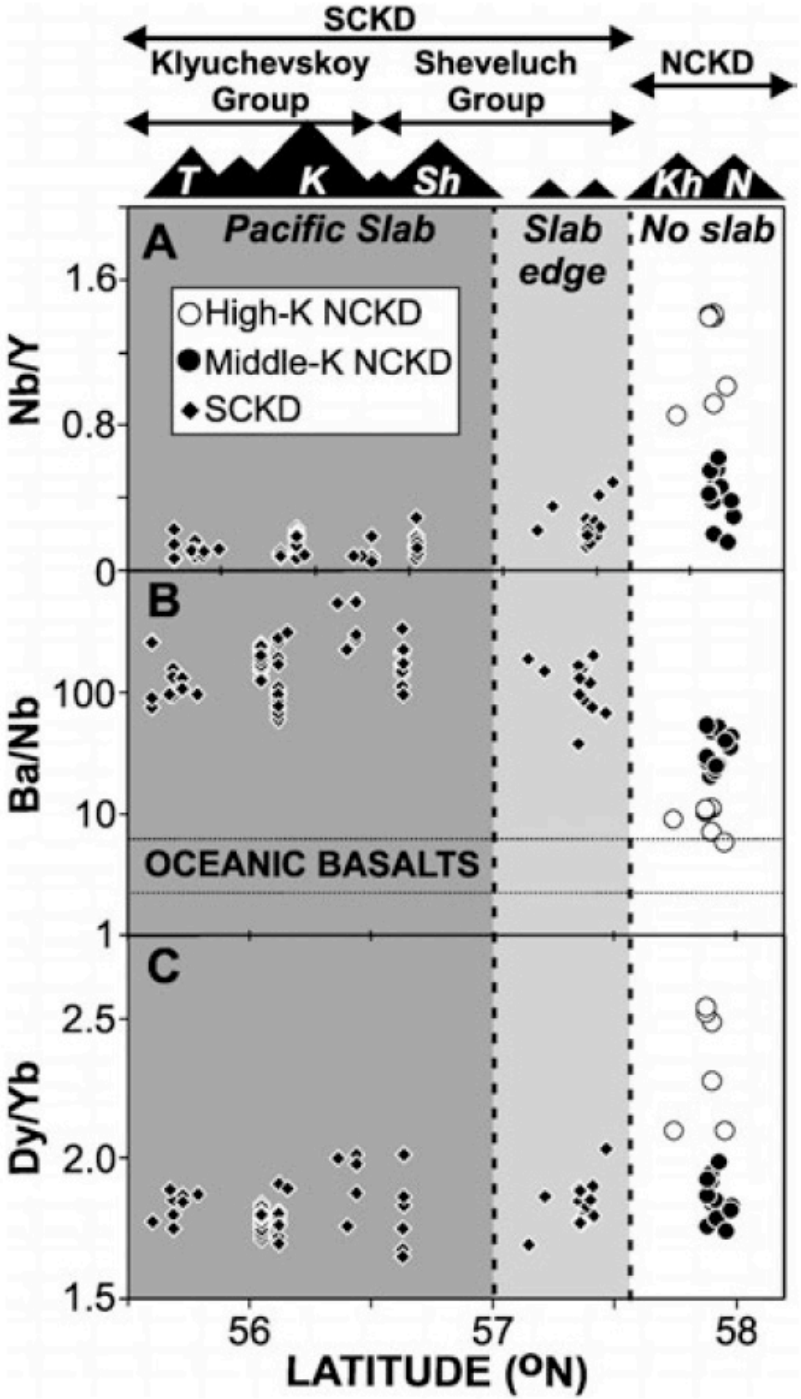

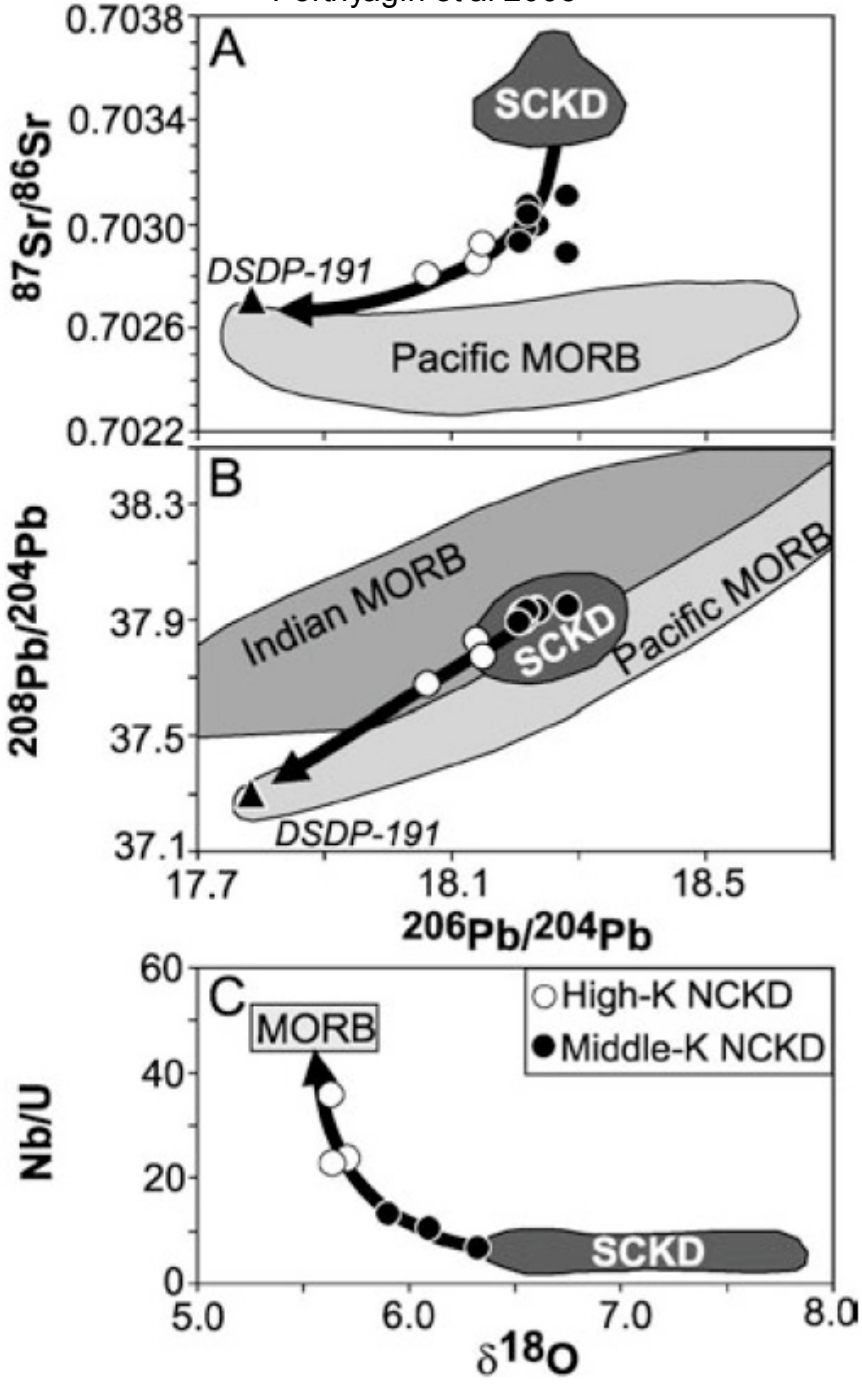

View to south

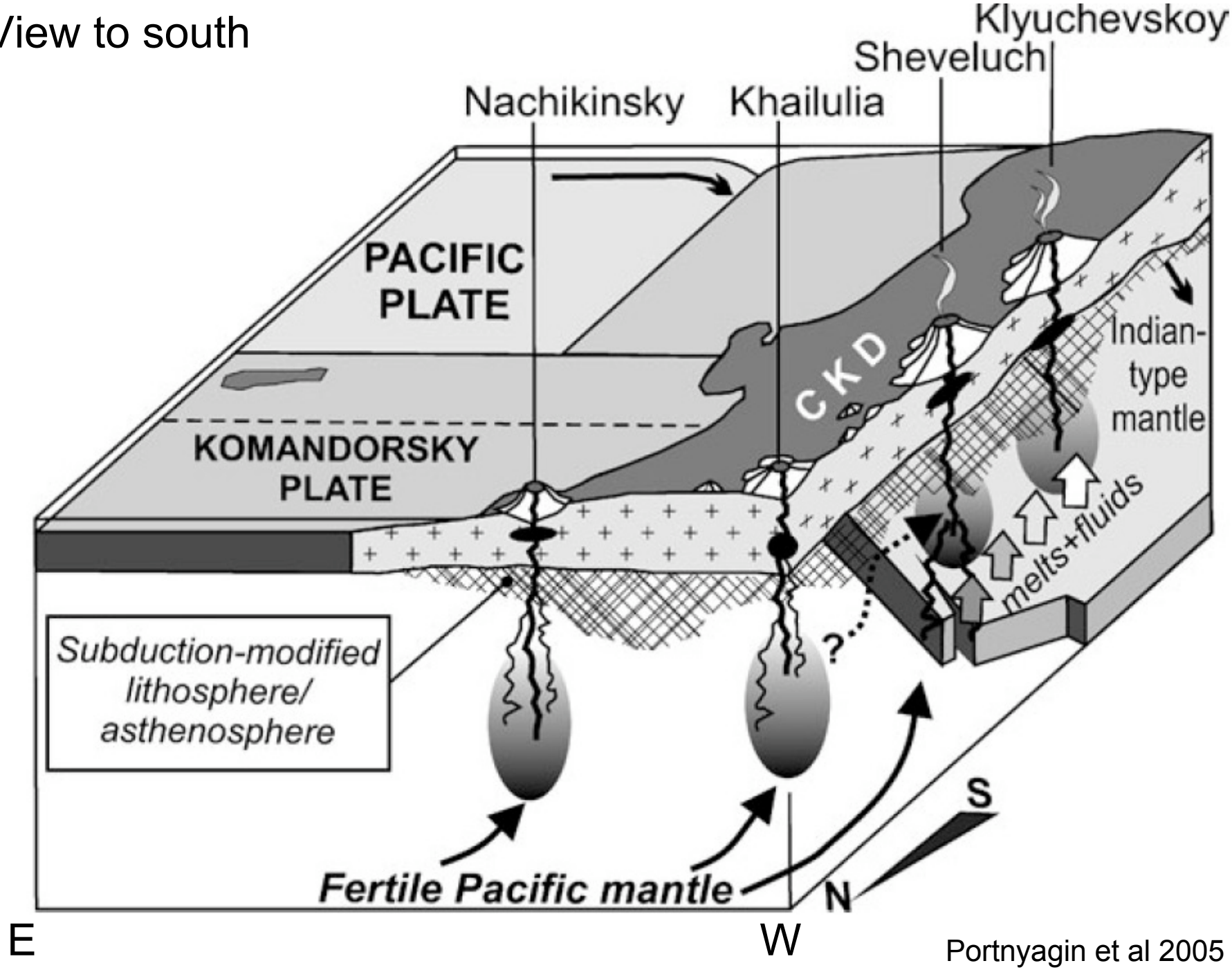

Portnyagin et al 2005

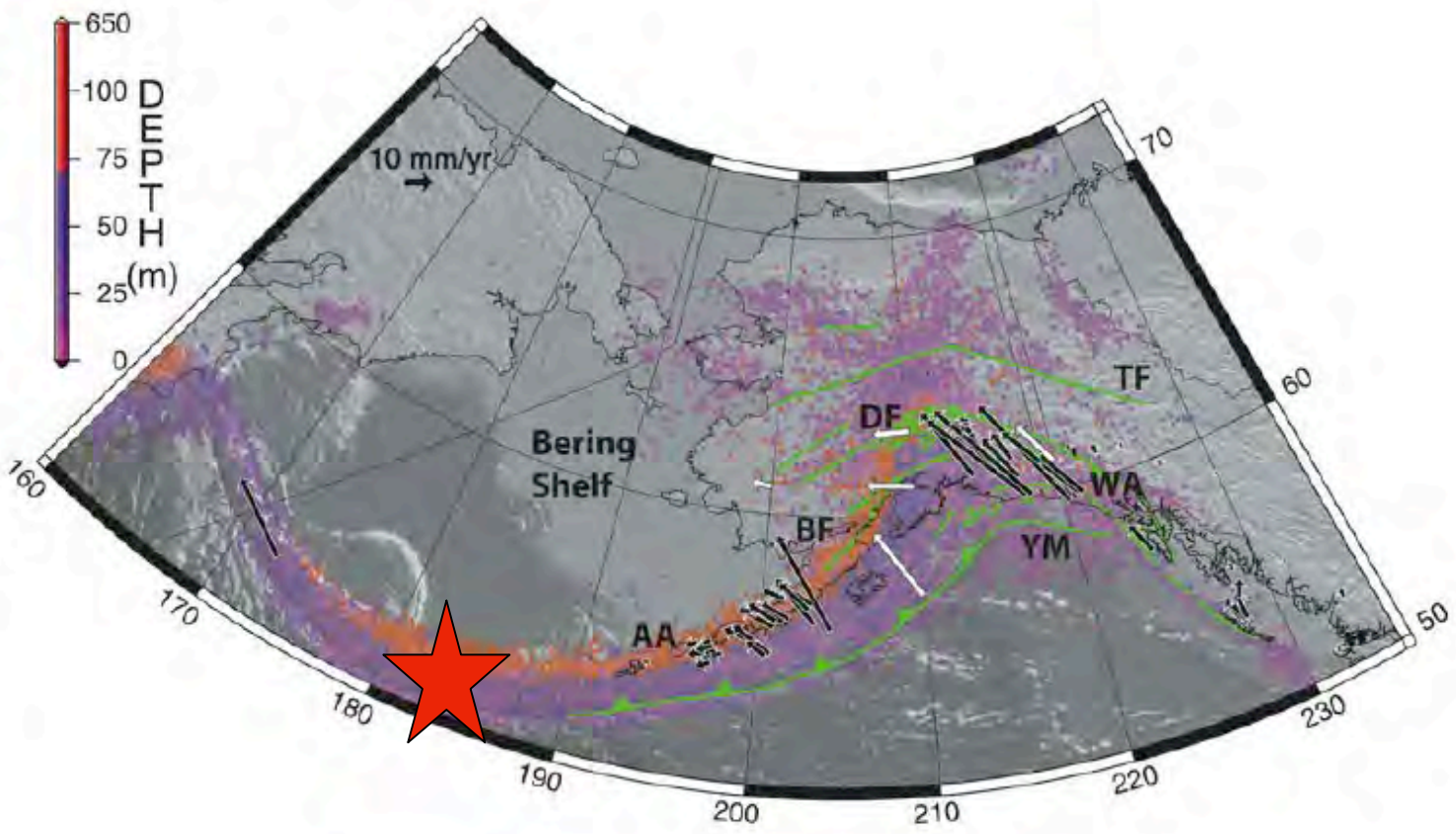

Figure 1. Southern Alaskan convergent margin. Green line segments denote major faults. Colored dots show locations of earthquakes >M_w = 3 from the Alaska Earthquake Information Center. Black vectors represent GPS observations from Sauber et al. (1997), Mazzotti et al. (2003), Fournier and Freymueller (2007), Fletcher and Freymueller (2003), and Avé Lallemant and Oldow (2000); white vectors show kinematic model velocities from Flesch et al. (2007). AA—Aleutian Arc; BF—Bruin Bay fault; TF—Tintina fault; DF—Denali fault; WR—Wrangell Arc; YM—Yakutat microplate.

Ridgeway and Flesch 2007

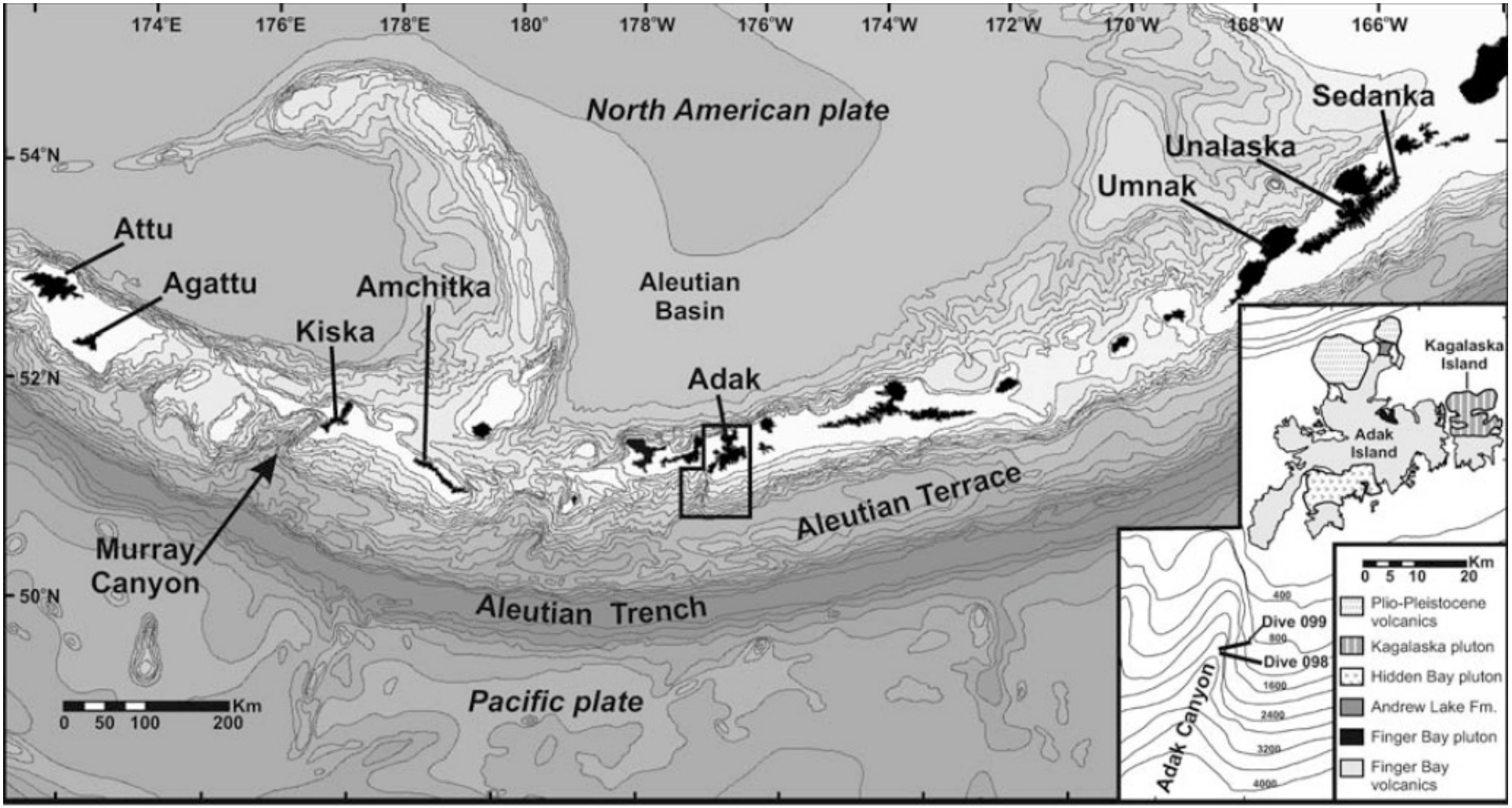

Jicha et al 2006

TABLE 1. SUMMARY OF $^{40}Ar/^{39}Ar$ INCREMENTAL HEATING EXPERIMENTS

Sample	Depth (m) or island	Material	# of expts.	^{39}Ar %	MSWD	$^{40}Ar/^{39}Ar_i$ ±2σ	Isochron age (Ma) ±2σ
Terrestrial volcanic and plutonic rocks							
AD 03 04	Adak	groundmass	1	100.0	0.16	296.7 ± 2.8	7.00 ± 0.24
		plagioclase	1	82.8	0.21	292.2 ± 15.0	7.90 ± 3.17
KAG7-32	Kagalaska	biotite	1	100.0	0.33	296.9 ± 6.3	14.14 ± 0.12
KAG7-50	Kagalaska	biotite	1	100.0	0.12	299.6 ± 13.1	14.24 ± 0.71
		hornblende	1	92.8	0.21	294.1 ± 24.7	14.66 ± 1.67
AM33	Amchitka	plagioclase	1	100.0	0.03	297.8 ± 6.2	15.36 ± 1.22
		hornblende	1	100.0	0.21	299.6 ± 27.8	15.30 ± 1.40
MR80-12	Adak	groundmass	1	100.0	0.45	295.9 ± 5.9	25.66 ± 0.69
AT80-87	Attu	plagioclase	2	88.9	0.19	296.3 ± 1.5	29.38 ± 1.48
SED-AB	Sedanka	hornblende	2	100.0	0.17	297.4 ± 2.7	29.68 ± 0.91
SED36-D	Sedanka	biotite	1	94.1	0.98	294.4 ± 10.8	30.32 ± 0.24
HB76-125	Adak	biotite	2	98.4	0.11	293.3 ± 5.9	34.50 ± 0.27
		hornblende	2	100.0	0.01	296.2 ± 3.2	34.75 ± 0.95
AT80-22	Attu	plagioclase	1	99.3	0.29	297.2 ± 2.2	34.69 ± 0.99
		hornblende	2	100.0	0.29	291.9 ± 10.5	35.37 ± 2.04
BW8-R39B	Adak	groundmass	1	100.0	1.02	302.9 ± 9.3	37.26 ± 0.74
MV80-24	Adak	plagioclase	2	91.7	0.50	299.5 ± 17.6	37.55 ± 1.00
FB8-19	Adak	biotite	1	100.0	0.92	293.2 ± 3.6	37.89 ± 0.23
Adak Canyon Dive 099							
J99S20S24	1281	groundmass	2	100.0	0.21	296.1 ± 9.7	32.90 ± 1.22
J99S13S19	1650	plagioclase	1	100.0	0.39	297.1 ± 2.2	32.89 ± 0.55
J99S12S18	1691	groundmass	1	99.2	0.66	295.1 ± 9.5	33.79 ± 0.29
J99S6S9	2021	groundmass	3	100.0	0.70	295.2 ± 11.3	36.12 ± 0.71
J99S4S7	2049	groundmass	1	100.0	0.09	295.3 ± 10.1	36.14 ± 0.48
J99S3S6	2119	plagioclase	2	100.0	0.10	296.0 ± 22.0	36.00 ± 1.50
J99S3S5	2119	groundmass	1	100.0	0.21	295.7 ± 5.9	35.87 ± 0.61
J99S2S4	2125	groundmass	2	100.0	0.01	301.0 ± 10.3	36.52 ± 0.91
J99S1S2	2203	groundmass	2	100.0	0.27	294.1 ± 7.1	36.65 ± 1.18
J99S1S1	2203	groundmass	1	100.0	0.46	297.6 ± 12.3	37.84 ± 0.86
Adak Canyon Dive 098							
J98S7S8	2035	groundmass	2	86.6	0.22	293.0 ± 2.4	28.69 ± 0.19
J98S6S7	2070	groundmass	2	100.0	0.42	297.1 ± 5.1	34.25 ± 0.51
J98S3S3	2715	groundmass	1	100.0	0.20	294.1 ± 4.6	30.38 ± 1.15
Murray Canyon Dredge							
TN182-30-001	2535	plagioclase	1	100.0	0.28	294.8 ± 1.9	22.06 ± 0.78
		biotite	1	100.0	0.22	294.7 ± 6.7	21.82 ± 1.28
TN182-30-003	3018	groundmass	3	69.2	1.20	292.3 ± 2.6	46.31 ± 0.91

Jicha et al 2006

TABLE 2. ESTIMATES OF MAGMA PRODUCTION RATES OVER THE LAST 46 m.y.

Model parameters	Volume (km^3/km)	Magma production rate ($km^3/km/my$)
Existing crustal material fully compacted:	5500	
6-km-thick remnant of the Kula plate in the mid-crust:	1400	
Material lost via subduction erosion @ 30 $km^3/km/m.y.$	1380	
Material lost via glacial and subaerial erosion	1500	
Model A: Existing arc material minus the Kula plate in mid-crust	4100	89
Model A + volume lost via subduction, glacial, and subaerial erosion:	6980	152
Model B: Existing arc material (no Kula plate in mid-crust):	5500	120
Model B + volume lost via subduction, glacial, and subaerial erosion:	8380	182

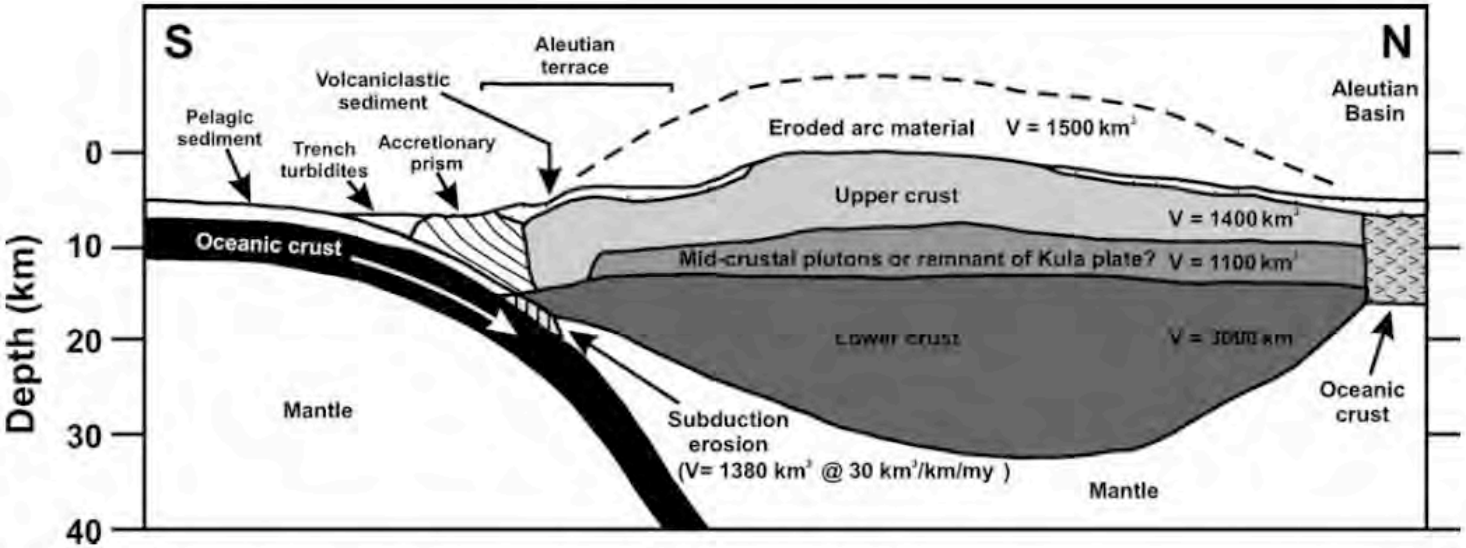

Figure 2. Cross section of central Aleutian Island Arc showing various components of the arc. Composition and volume of each layer are based on the P-wave velocity models of Holbrook et al. (1999) and Lizarralde et al. (2002). Erosional estimates are described in the text.

Jicha et al 2006

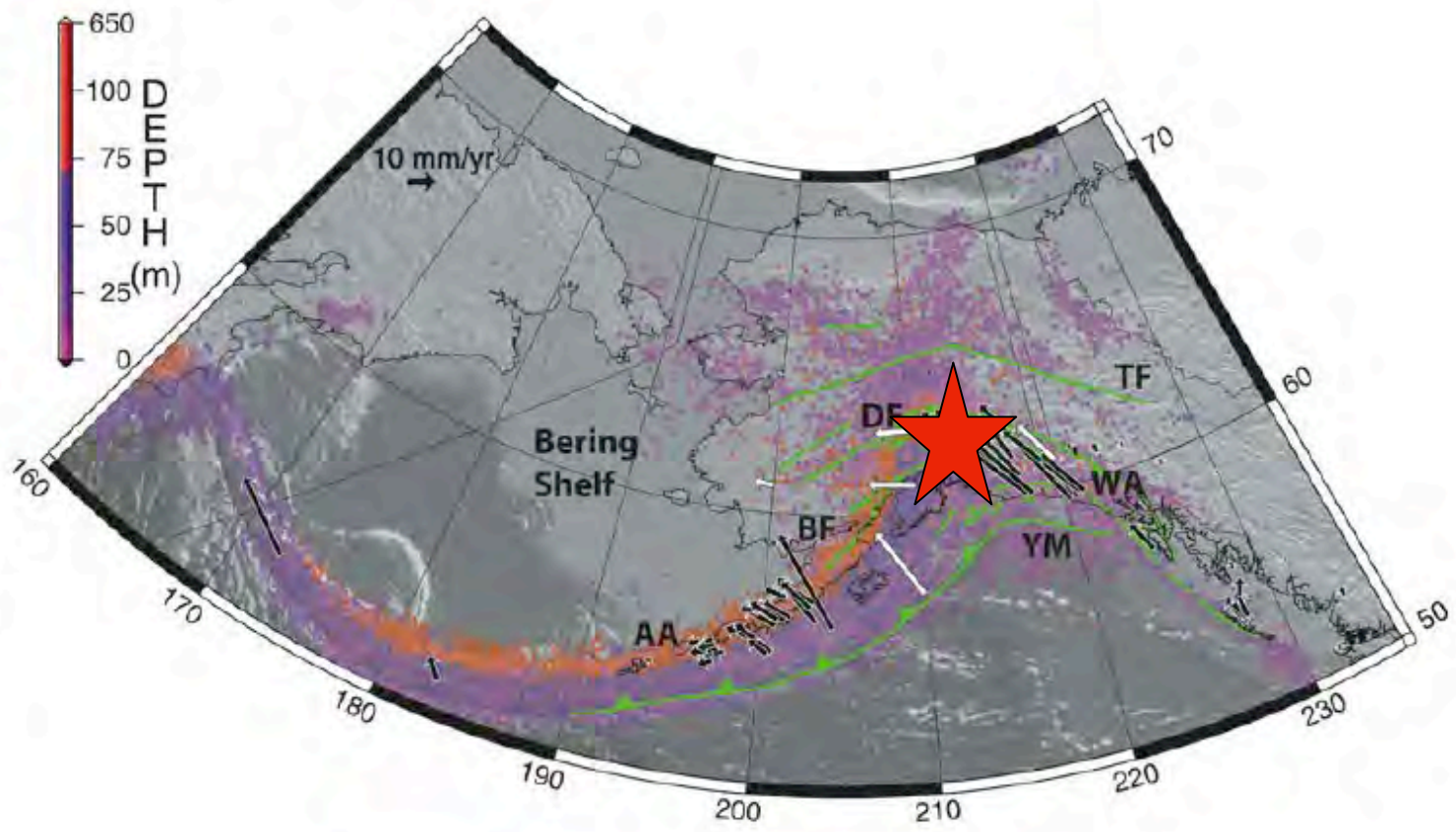

Figure 1. Southern Alaskan convergent margin. Green line segments denote major faults. Colored dots show locations of earthquakes >M_w = 3 from the Alaska Earthquake Information Center. Black vectors represent GPS observations from Sauber et al. (1997), Mazzotti et al. (2003), Fournier and Freymueller (2007), Fletcher and Freymueller (2003), and Avé Lallemant and Oldow (2000); white vectors show kinematic model velocities from Flesch et al. (2007). AA—Aleutian Arc; BF—Bruin Bay fault; TF—Tintina fault; DF—Denali fault; WR—Wrangell Arc; YM—Yakutat microplate.

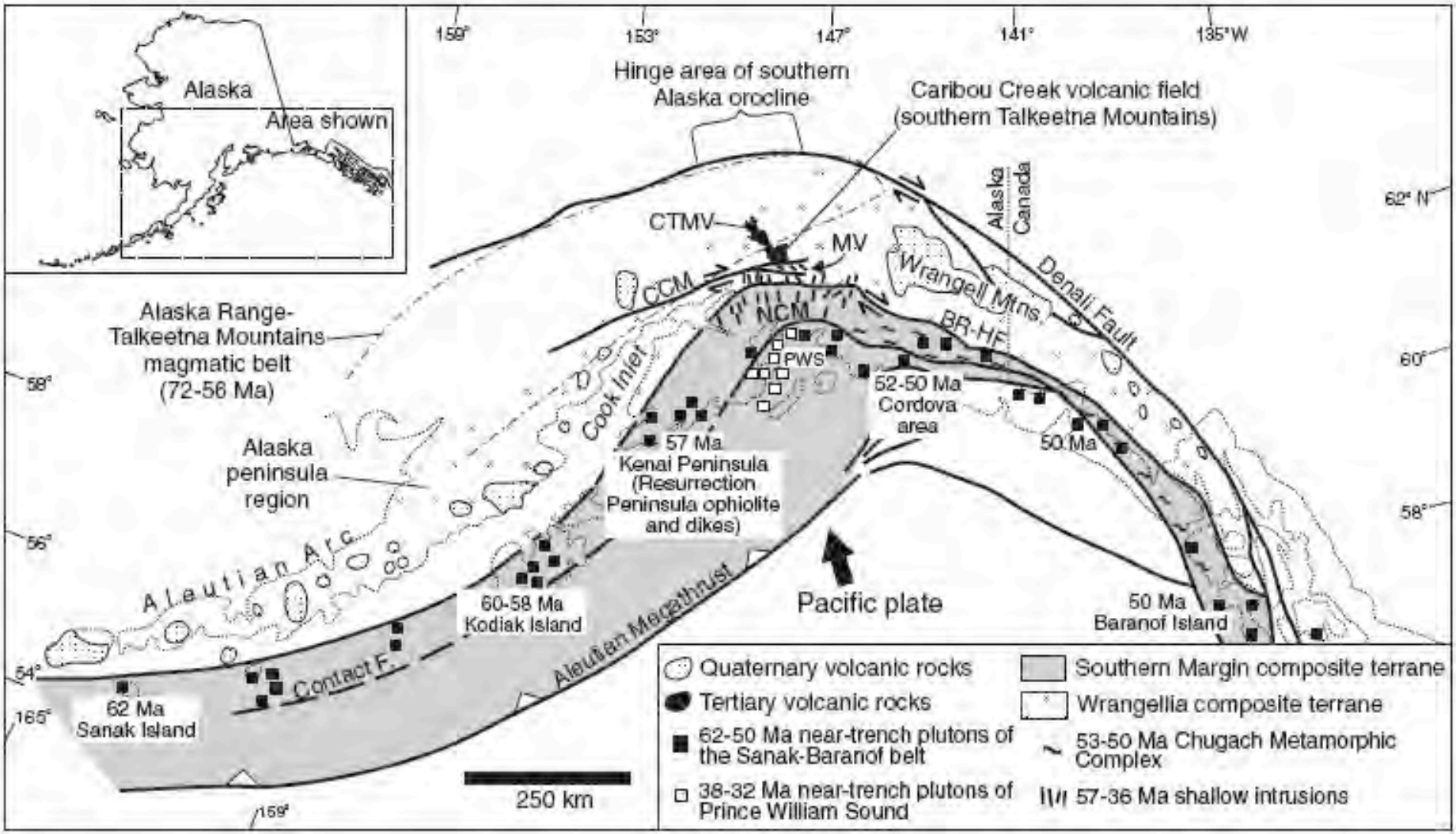

Cole et al 2006

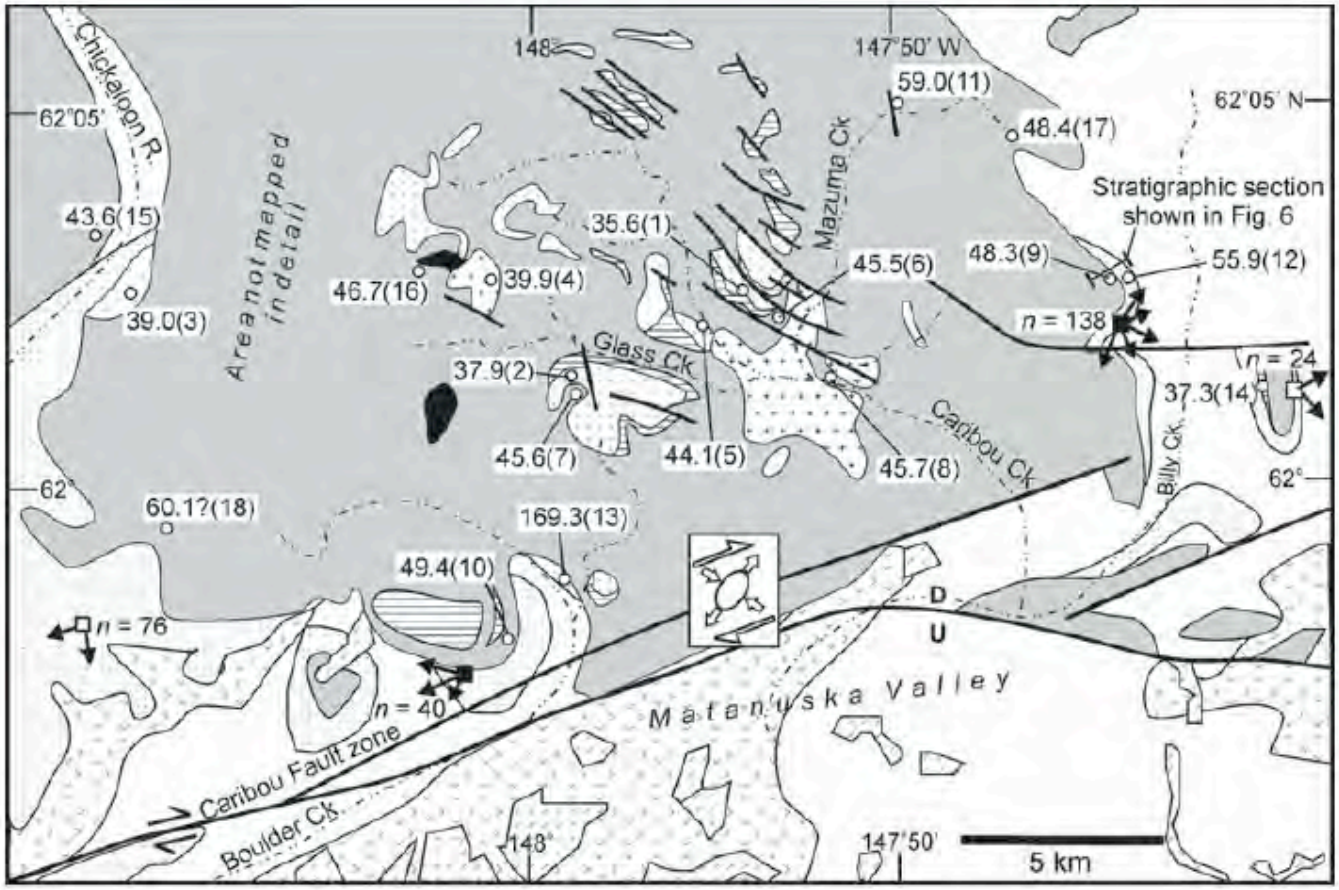

Caribou Creek volcanic rocks

- Rhyolite lavas, breccias, intrusives
- Dacite stocks
- Felsic and mafic pyroclastic deposits
- Mafic intrusion
- Mafic and intermediate lavas

- Tertiary mafic and felsic intrusions of the Matanuska Valley
- Tertiary conglomerate and sandstone (Wishbone Formation)
- Jurassic and Cretaceous sedimentary rocks
- Jurassic volcanic rocks (Talkeetna arc)

45.5(1) Radiometric age sample in Ma (parentheses show map number listed on Table 1)

Paleoflow data:

- Conglomerate clast imbrication (this study)
- Conglomerate clast imbrication (Trop et al., 2003)

Fault with predominant normal slip unless otherwise noted

Cole et al 2006

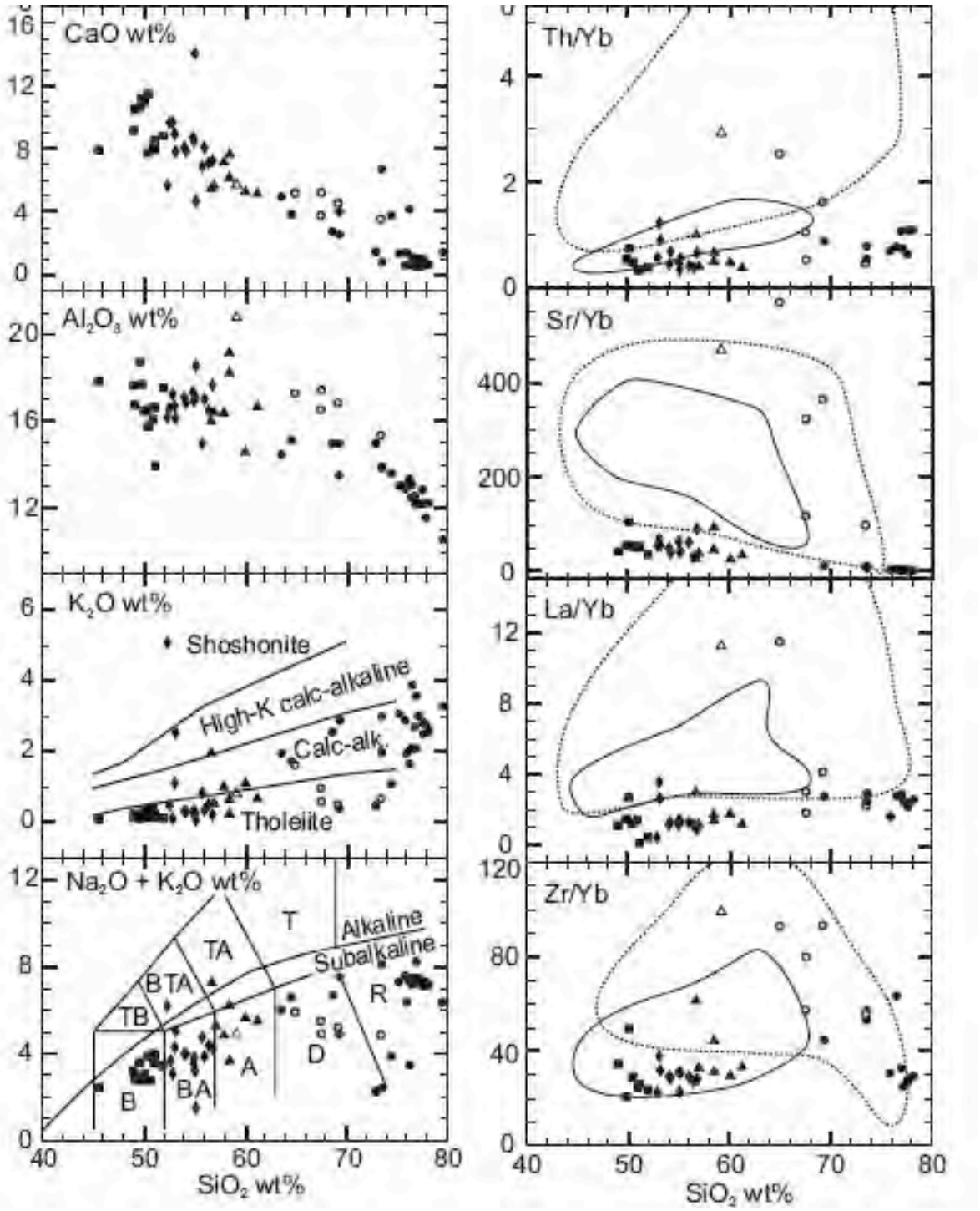
CaO wt%
Al_2O_3 wt%
K_2O wt%
Shoshonite
High-K calc-alkaline
Calc-alk
Tholeiite
$Na_2O + K_2O$ wt%
T
TA
BTA
TB
B
BA
A
D
R
Alkaline
Subalkaline
SiO_2 wt%
Th/Yb
Sr/Yb
La/Yb
Zr/Yb
SiO_2 wt%

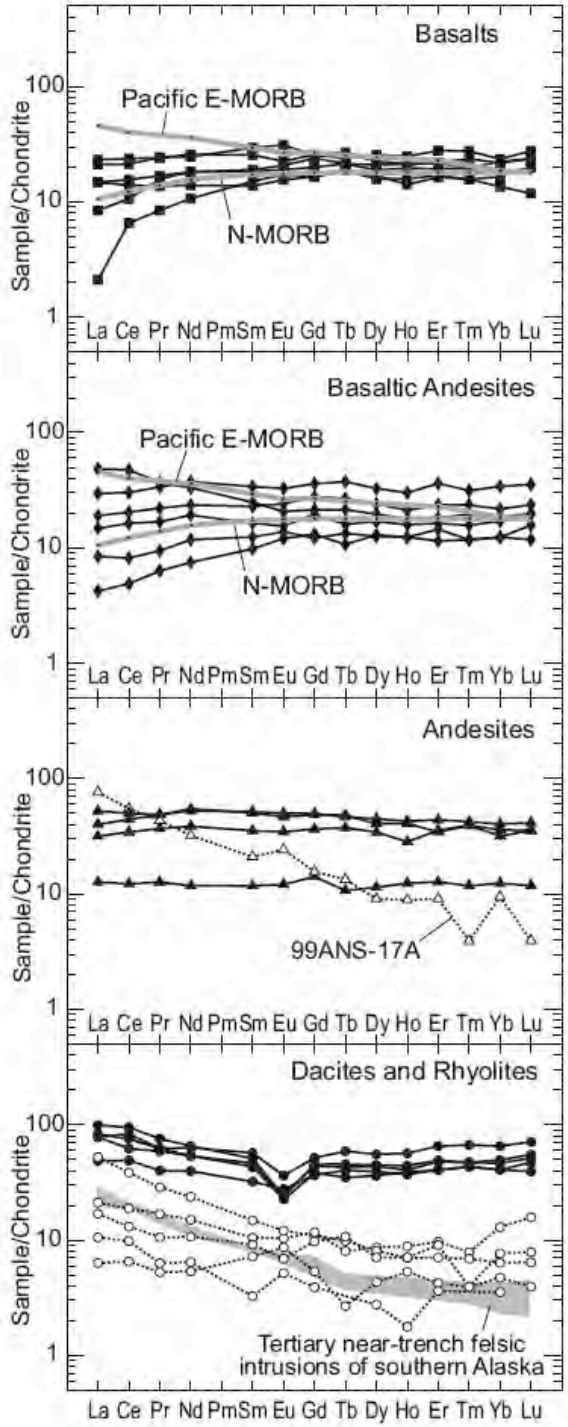
Basalts
Pacific E-MORB
N-MORB
Basaltic Andesites
Pacific E-MORB
N-MORB
Andesites
99ANS-17A
Dacites and Rhyolites
Tertiary near-trench felsic intrusions of southern Alaska
Sample/Chondrite
La Ce Pr Nd Pm Sm Eu Gd Tb Dy Ho Er Tm Yb Lu

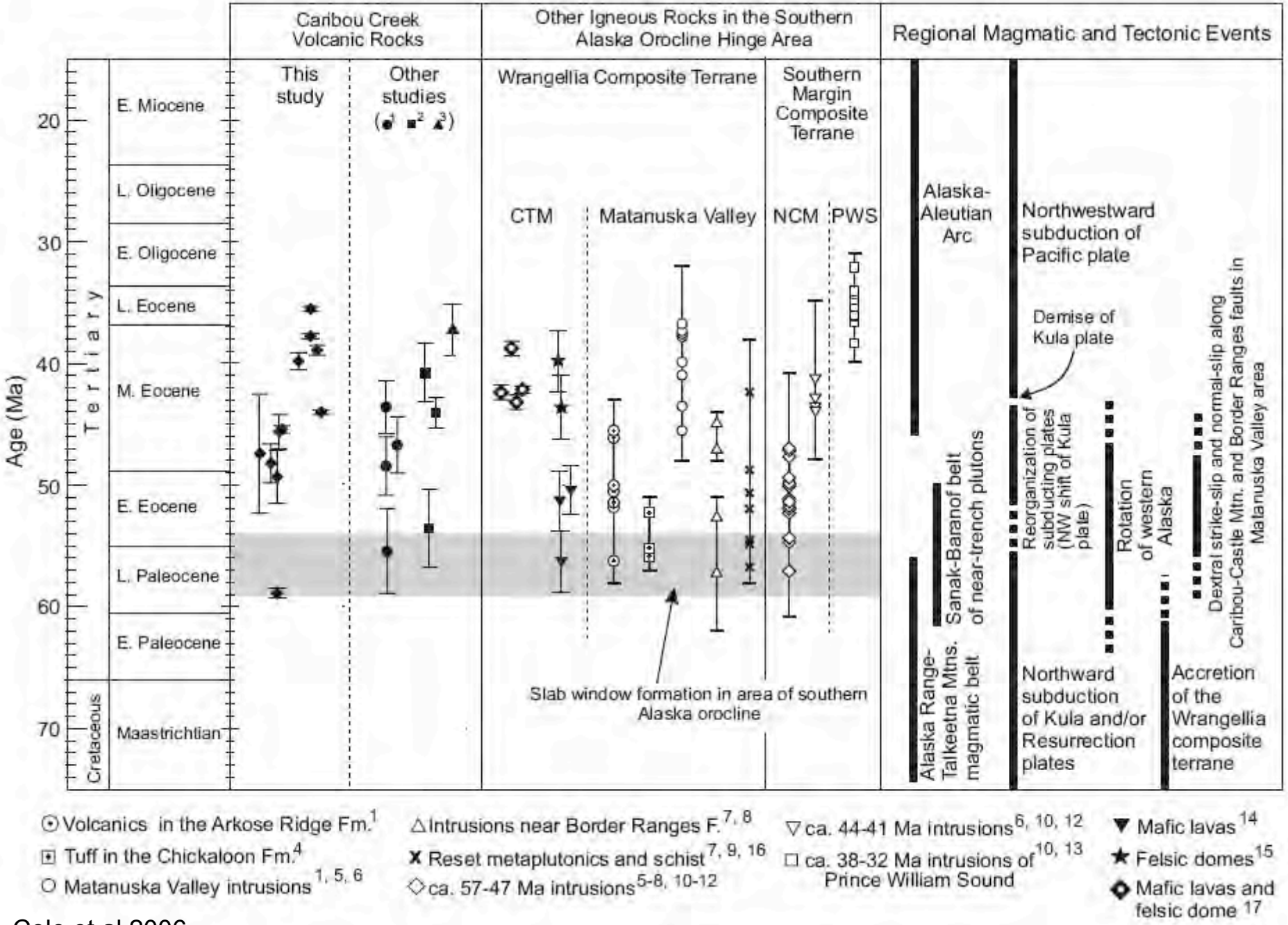

Cole et al 2006

Cole et al 2006

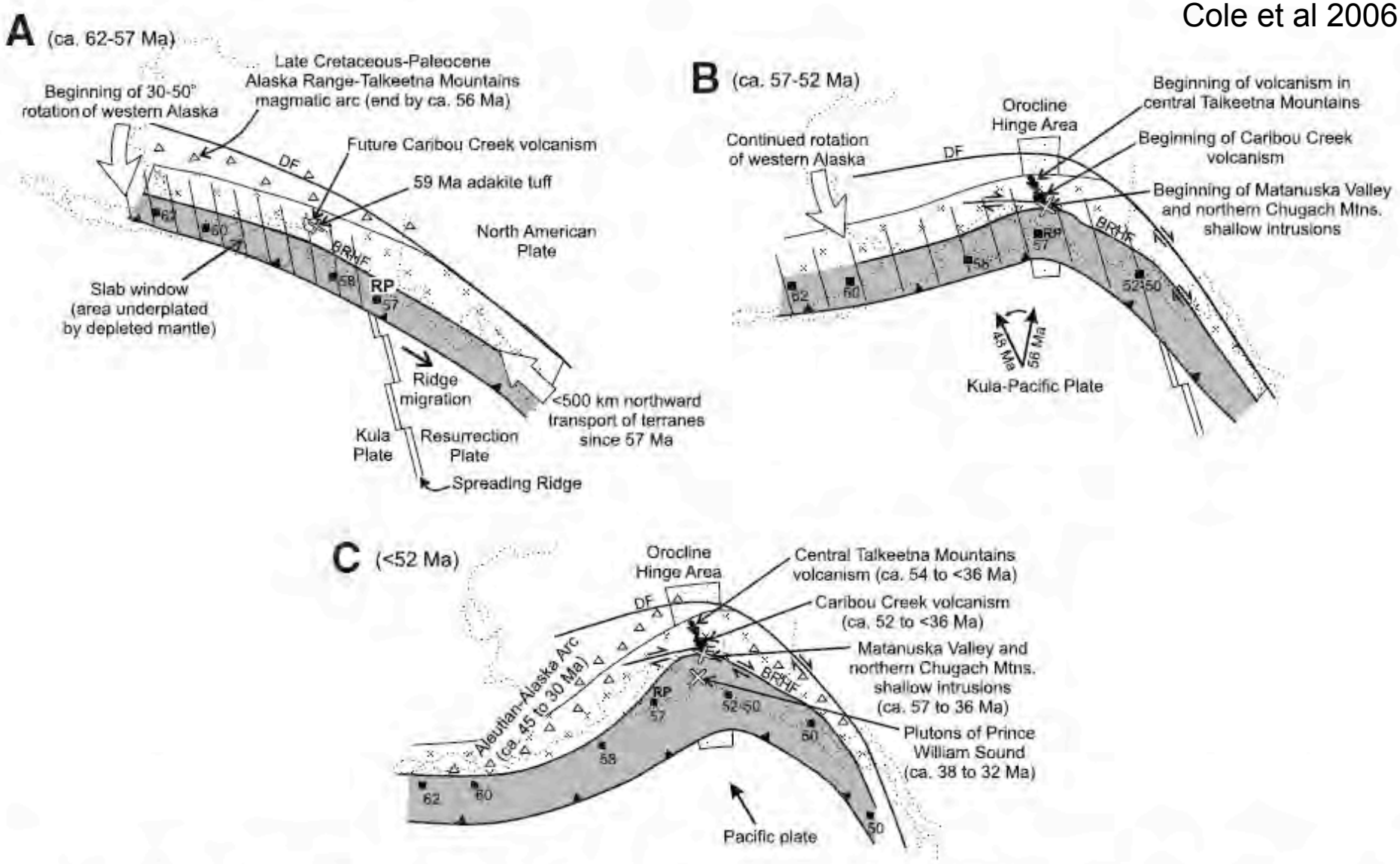

Figure 14. Tectonic reconstructions for southern Alaska, based on reconstructions of Wallace and Engebretson (1984), Engebretson et al. (1985), Lonsdale (1988), Bol et al. (1992), and Haeussler et al. (2003b). The restored position of the Southern Margin composite terrane (shaded region) is based upon the 95% minimum confidence limit of paleomagnetic data of Bol et al. (1992) and data of Kusky and Young (1999) for the Resurrection Peninsula ophiolite. The restored position of the Wrangellia composite terrane (x pattern) is based upon the combined paleomagnetic data of Hillhouse et al. (1985), Panuska et al. (1990), and Stamatakos et al. (2001). Representative near-trench

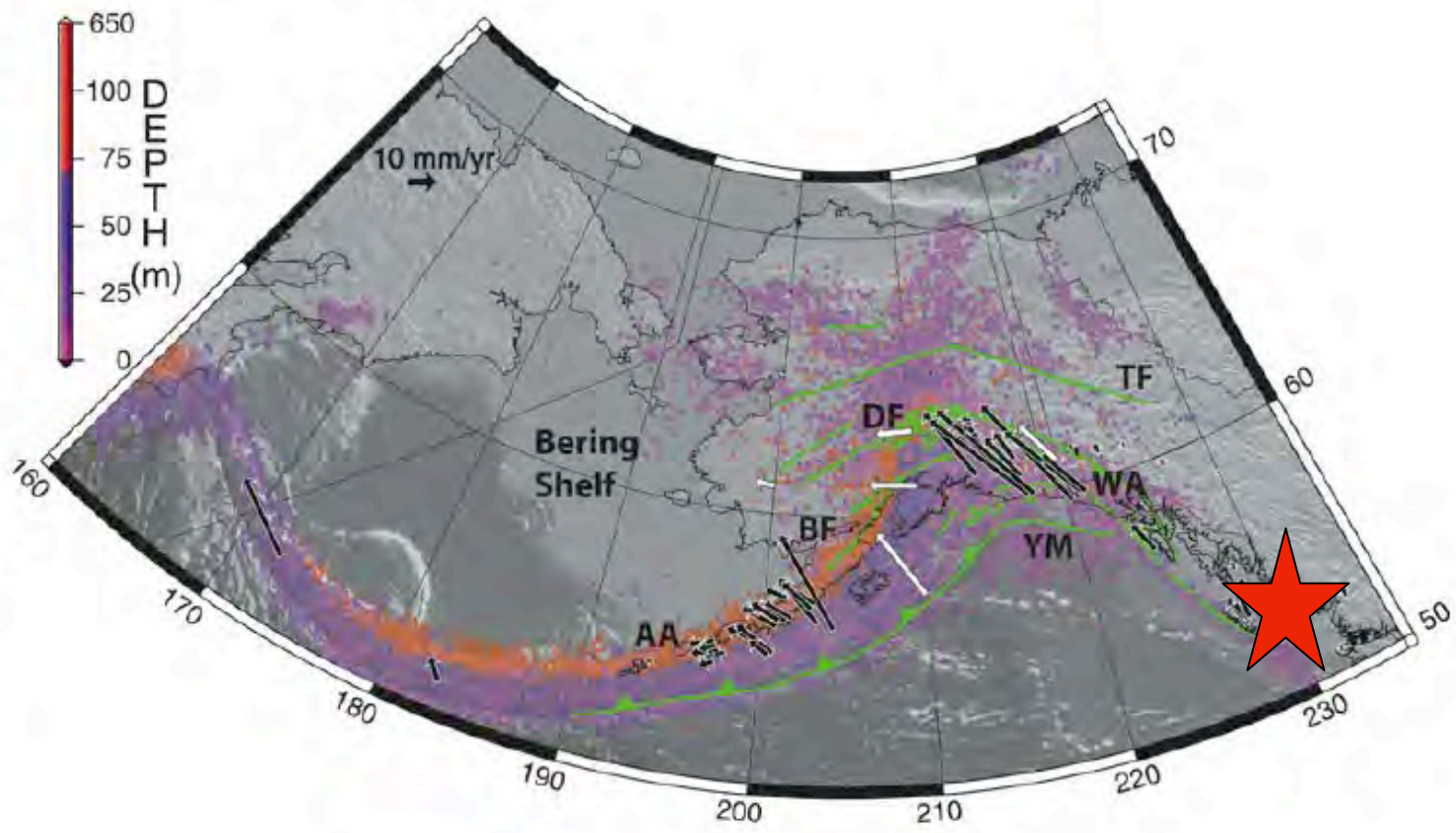

Figure 1. Southern Alaskan convergent margin. Green line segments denote major faults. Colored dots show locations of earthquakes >M_w = 3 from the Alaska Earthquake Information Center. Black vectors represent GPS observations from Sauber et al. (1997), Mazzotti et al. (2003), Fournier and Freymueller (2007), Fletcher and Freymueller (2003), and Avé Lallemant and Oldow (2000); white vectors show kinematic model velocities from Flesch et al. (2007). AA—Aleutian Arc; BF—Bruin Bay fault; TF—Tintina fault; DF—Denali fault; WR—Wrangell Arc; YM—Yakutat microplate.

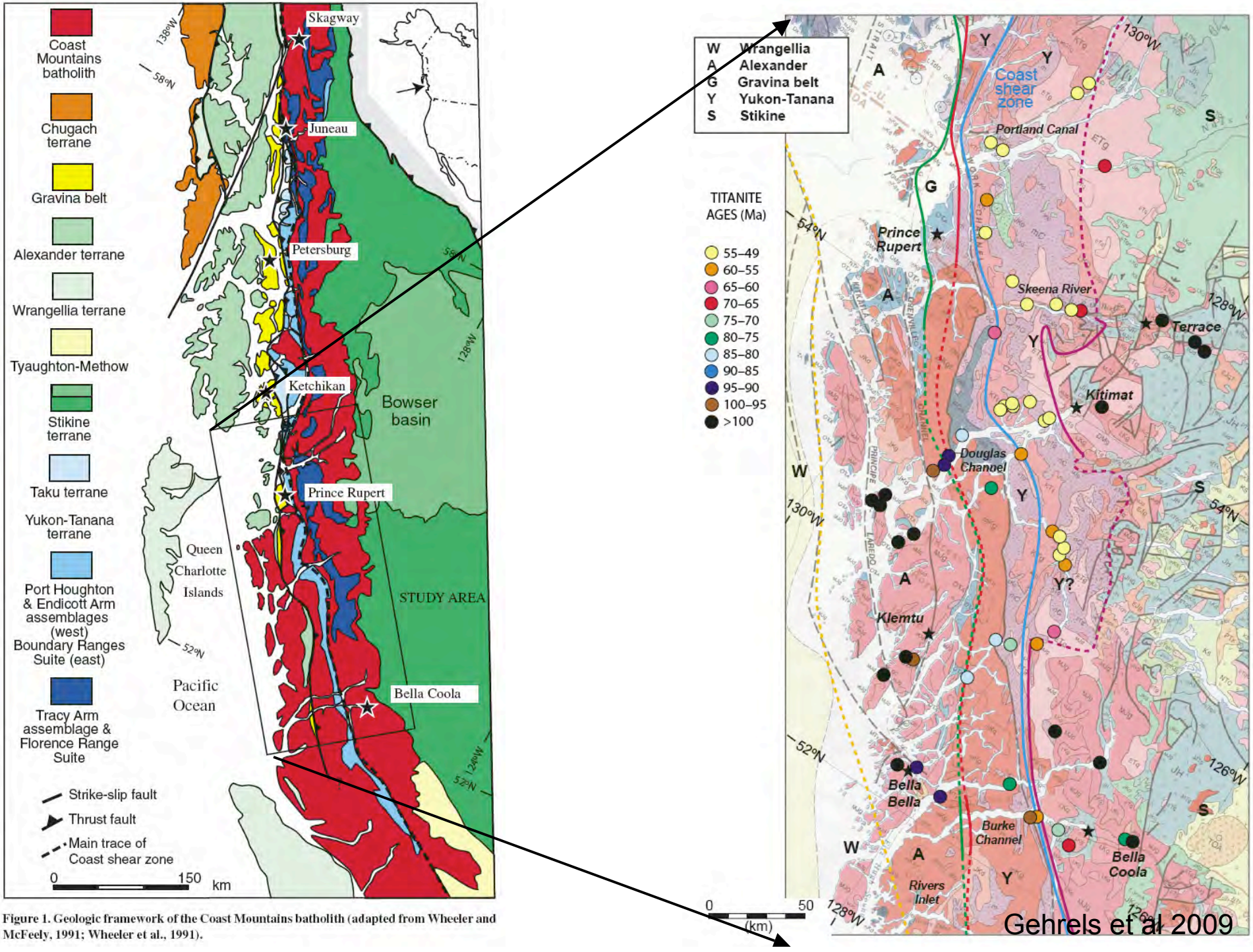

Figure 1. Geologic framework of the Coast Mountains batholith (adapted from Wheeler and McFeely, 1991; Wheeler et al., 1991).

Gehrels et al 2009

Gehrels et al 2009

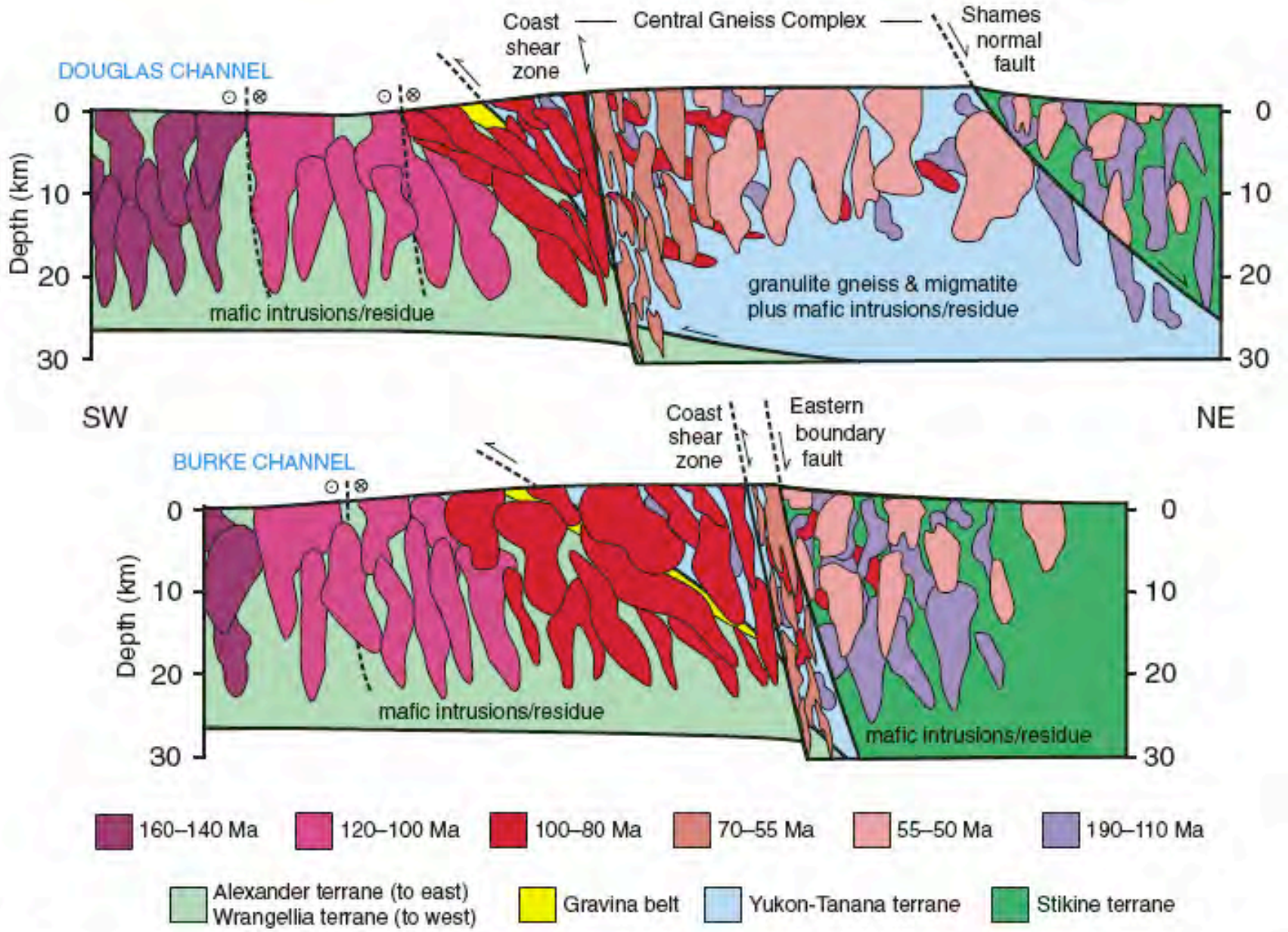

Figure 5. Schematic cross sections of the Coast Mountains batholith at latitudes of Douglas Channel (Kitimat) and Burke Channel (Bella Bella and Bella Coola). Geologic relations are

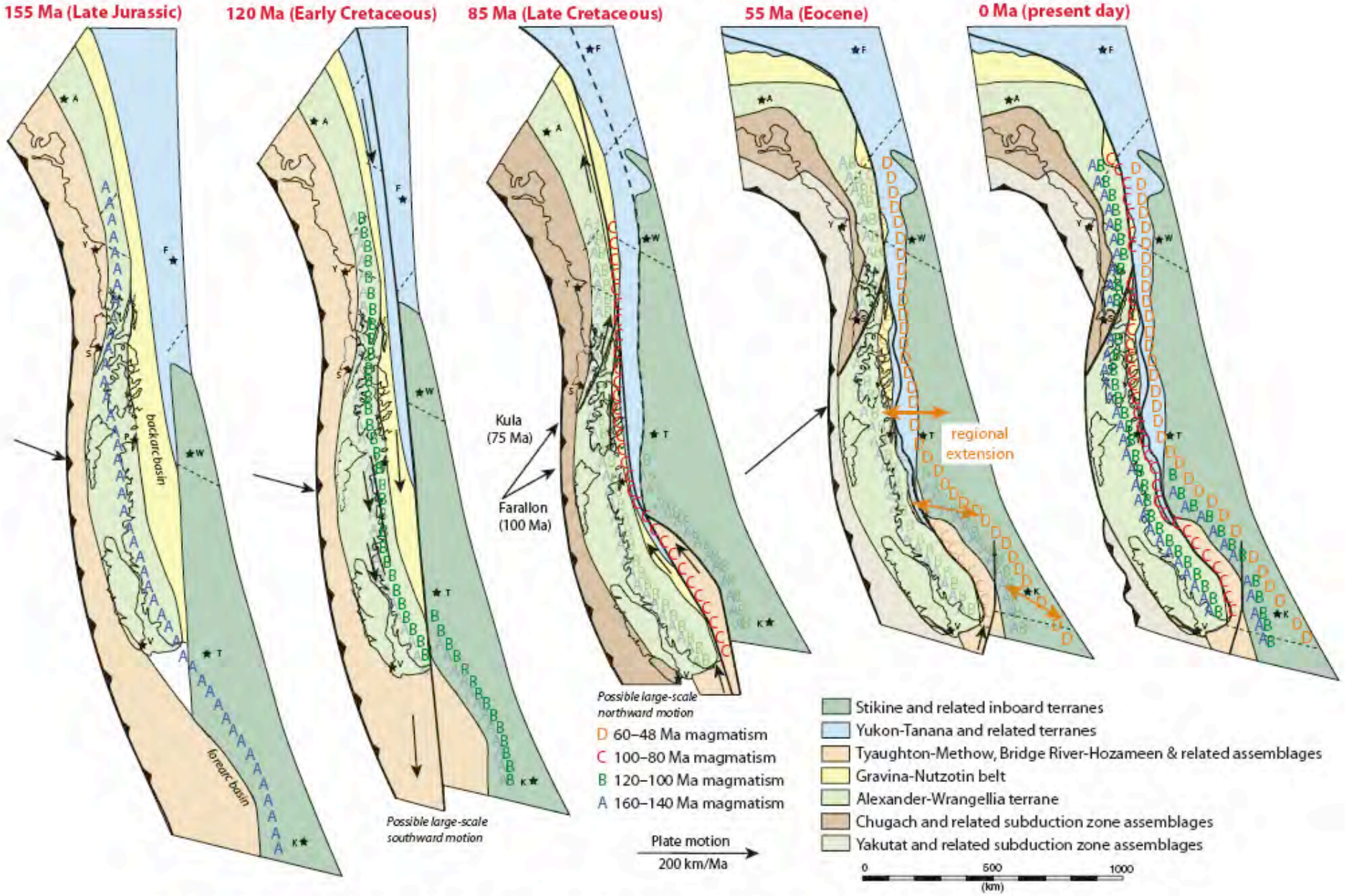

Figure 12. Schematic model offered for the tectonic evolution of the southern Coast Mountains batholith. Plate motion vectors are from Engebretson et al. (1985). See text for discussion.

Gehrels et al 2009

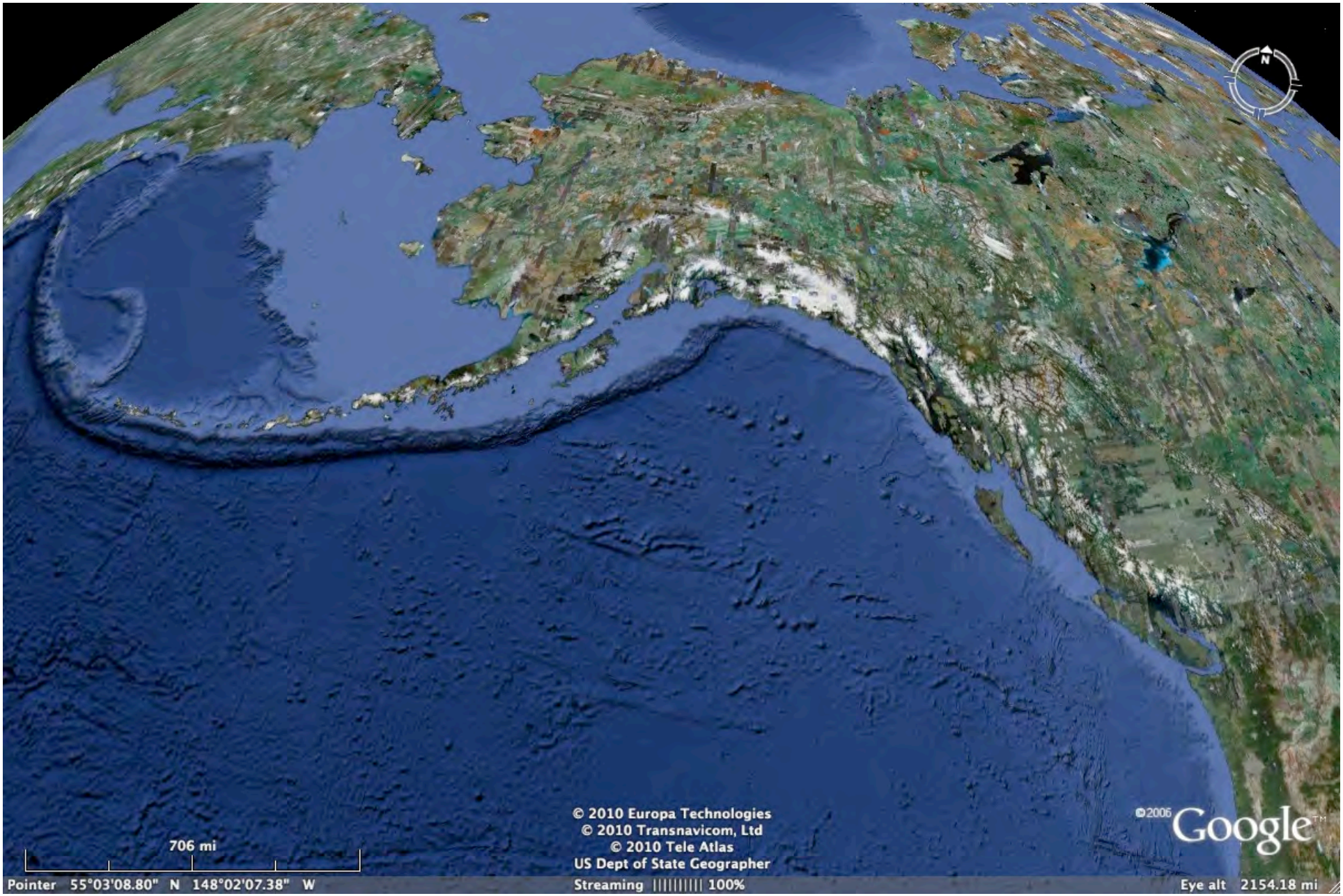
N
706 mi
© 2010 Europa Technologies
© 2010 Transnavicom, Ltd
© 2010 Tele Atlas
US Dept of State Geographer
©2006 Google™
Pointer 55°03'08.80" N 148°02'07.38" W
Streaming 100%
Eye alt 2154.18 mi

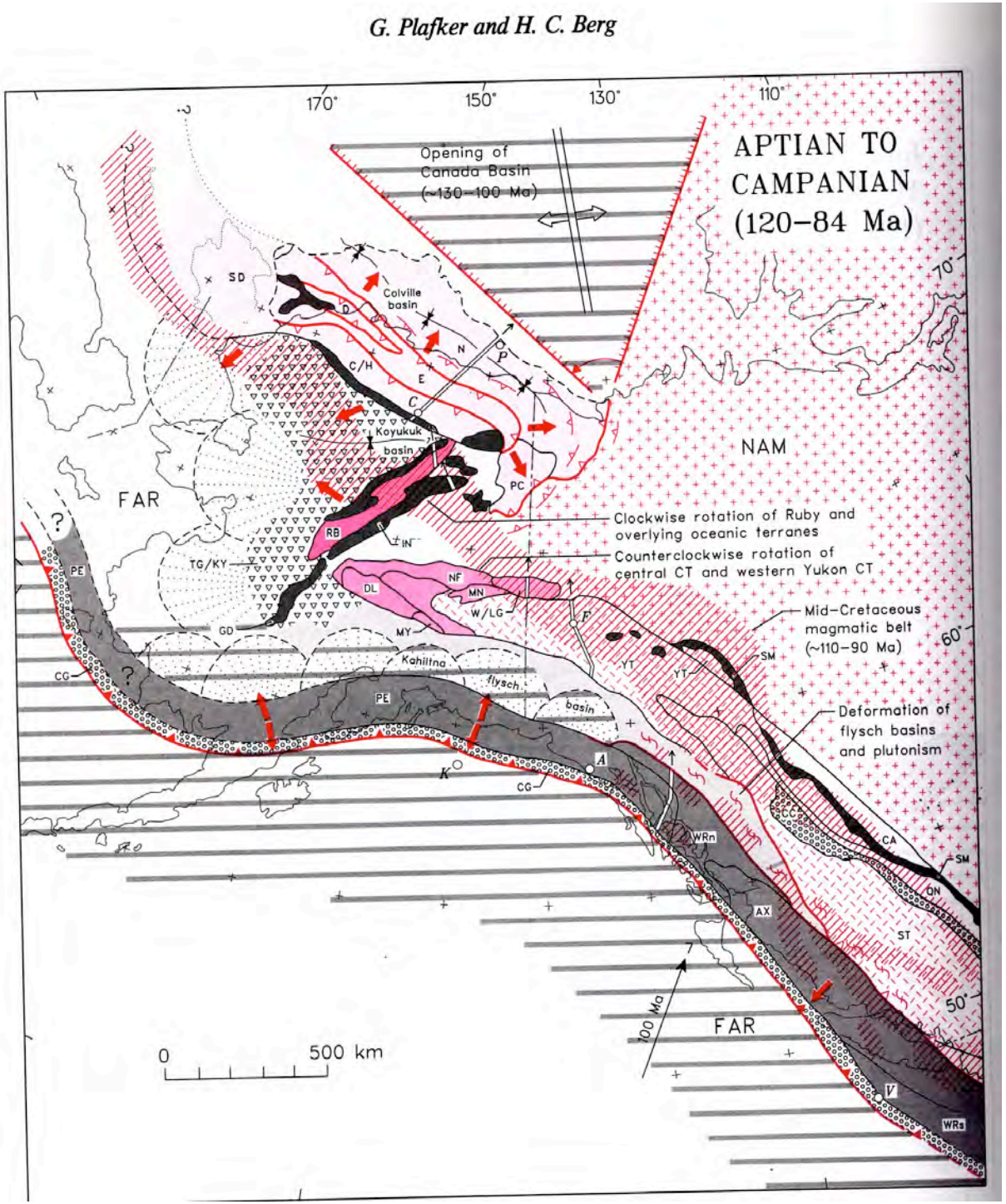

Pflaker and Bird 1994

Pflaker and
Bird 1994

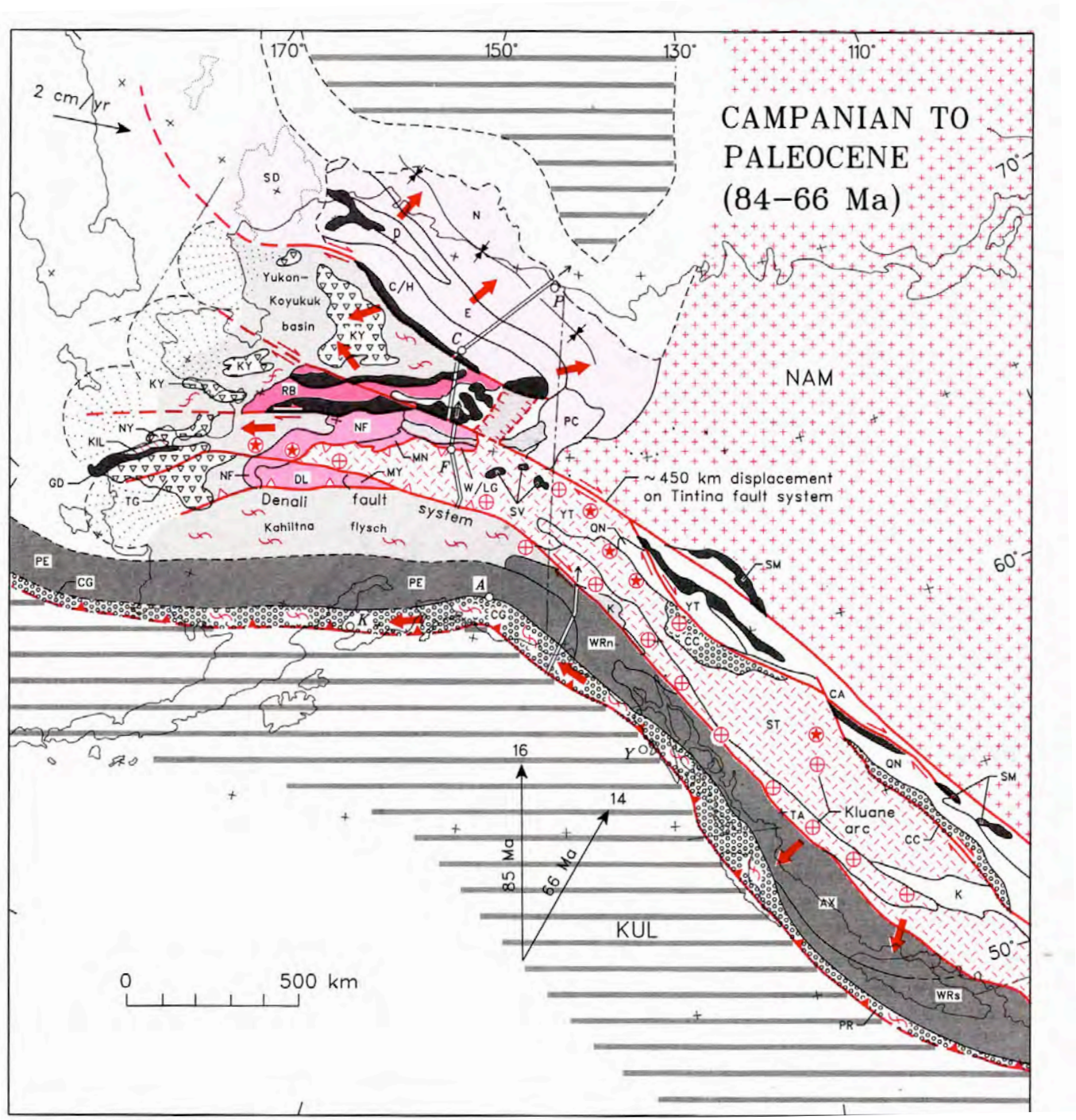

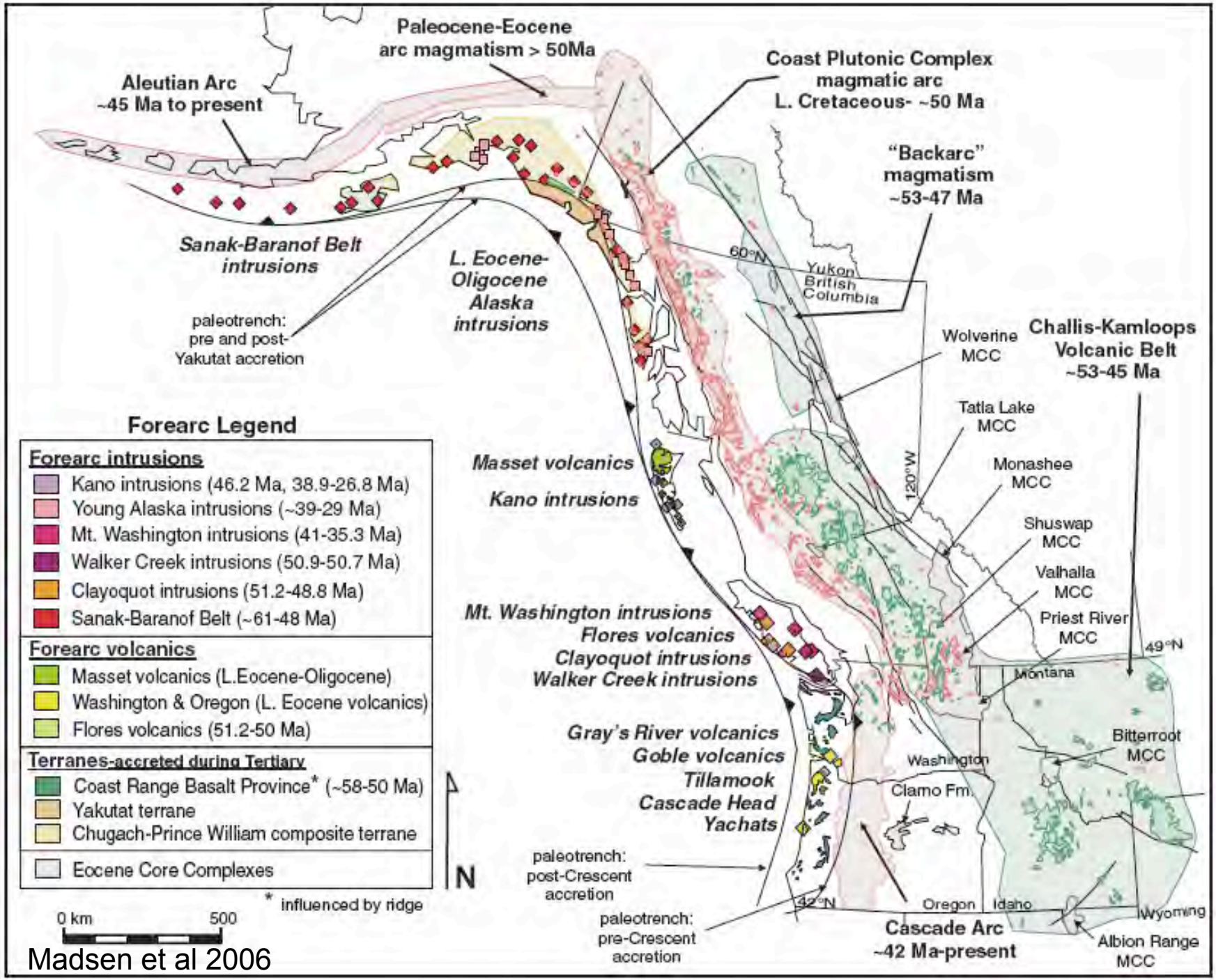

Madsen et al 2006

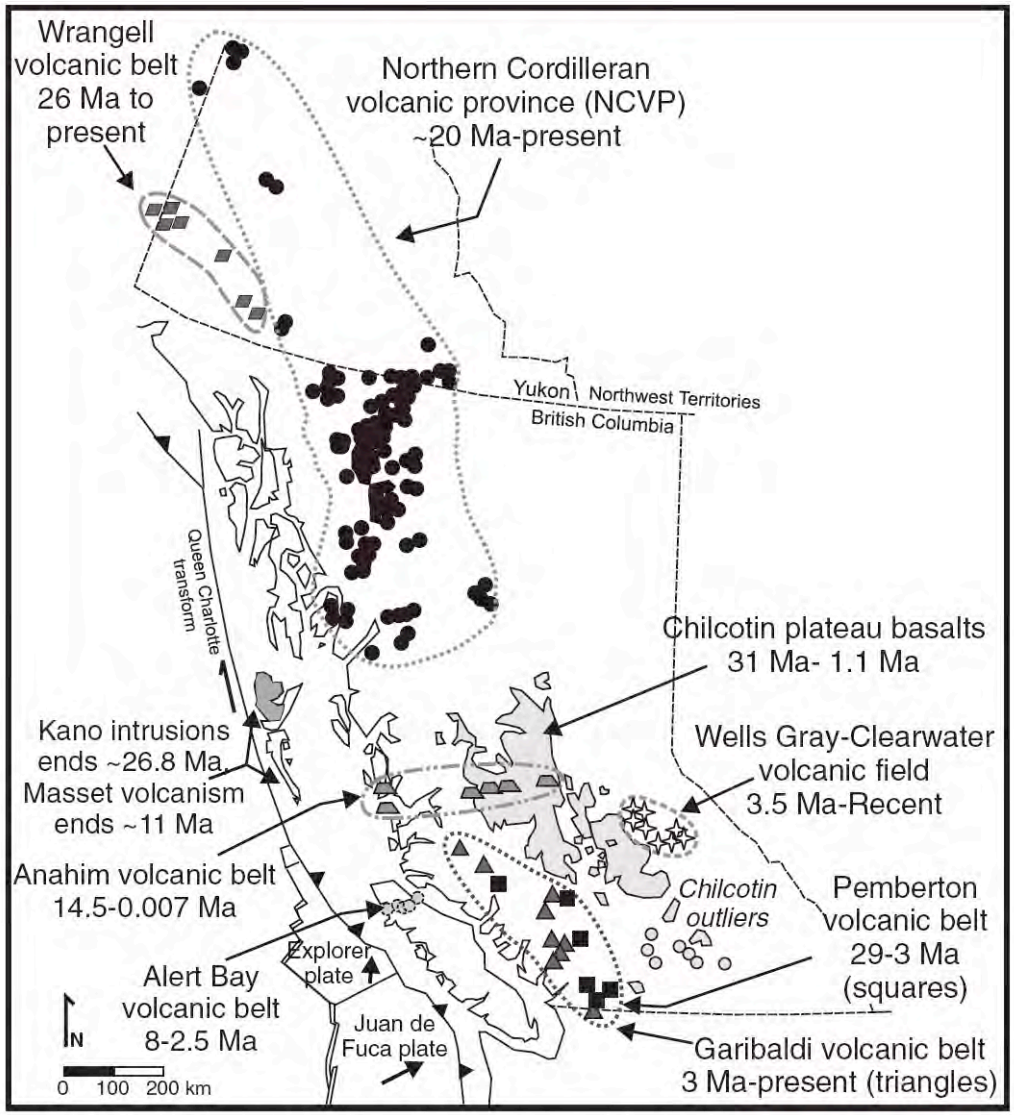

Figure 11. Late Oligocene to present forearc, arc, and within-plate magmatism in British Columbia, Yukon, and southeast Alaska. Volcanic fields are outlined. Individual volcanic centers of the northern Cordilleran volcanic province, Anahim belt, Wells Gray–Clearwater, and Wrangell fields are depicted by shapes within outlined fields. The Chilcotin Plateau is represented by the gray field in interior British Columbia. Arc magmatism is represented by squares and triangles of the Pemberton and Garibaldi belts, respectively. Oligocene to present forearc magmatism is found on Queen Charlotte Islands (Kano intrusions and Masset volcanics) and northern Vancouver Island (Alert Bay volcanic belt). The volcanic fields are described in the text. This figure is provided for comparison with the late Oligocene to present slab window reconstructions in Figures 10 and 12–14.

Madsen et al 2006

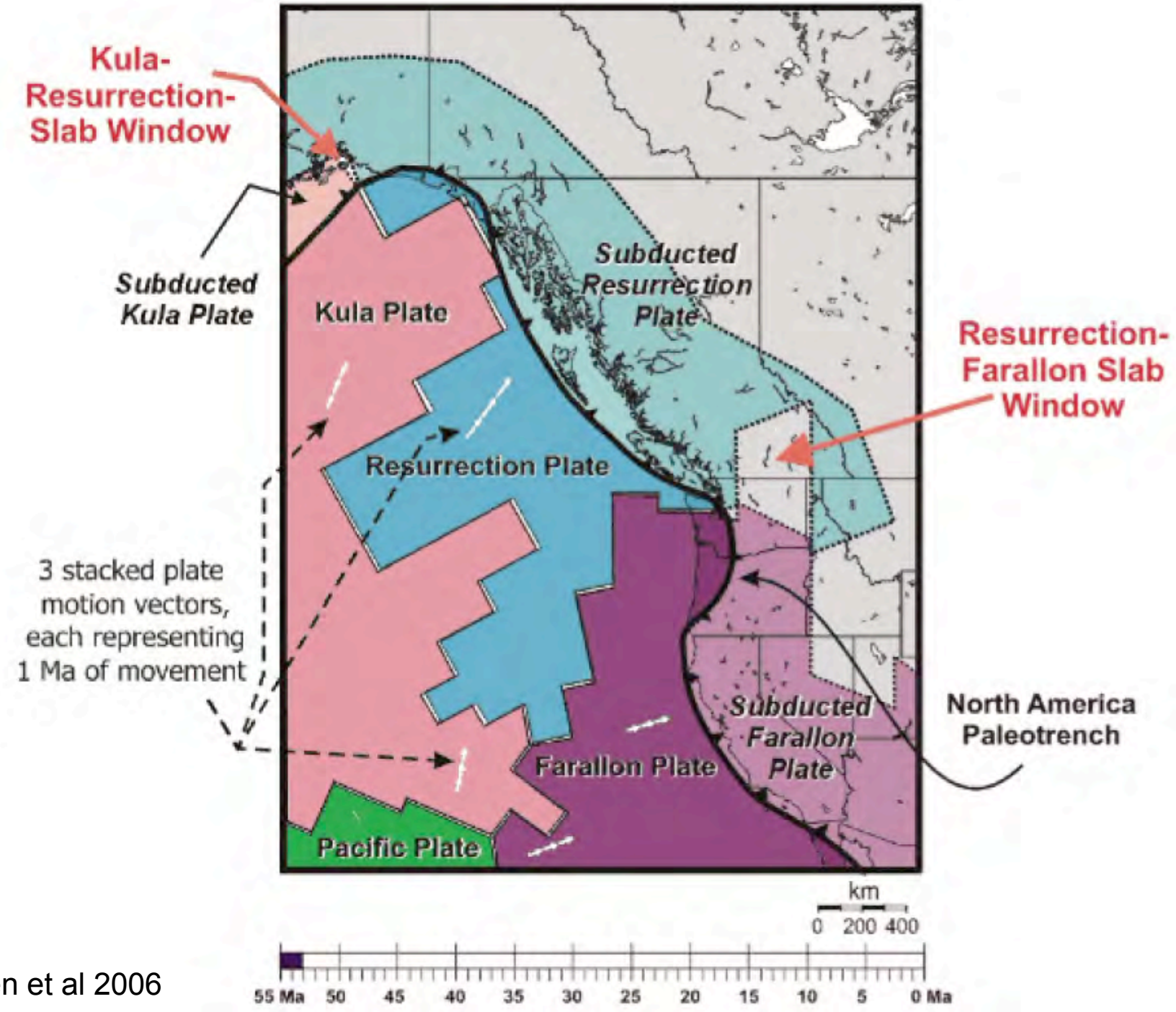

Madsen et al 2006

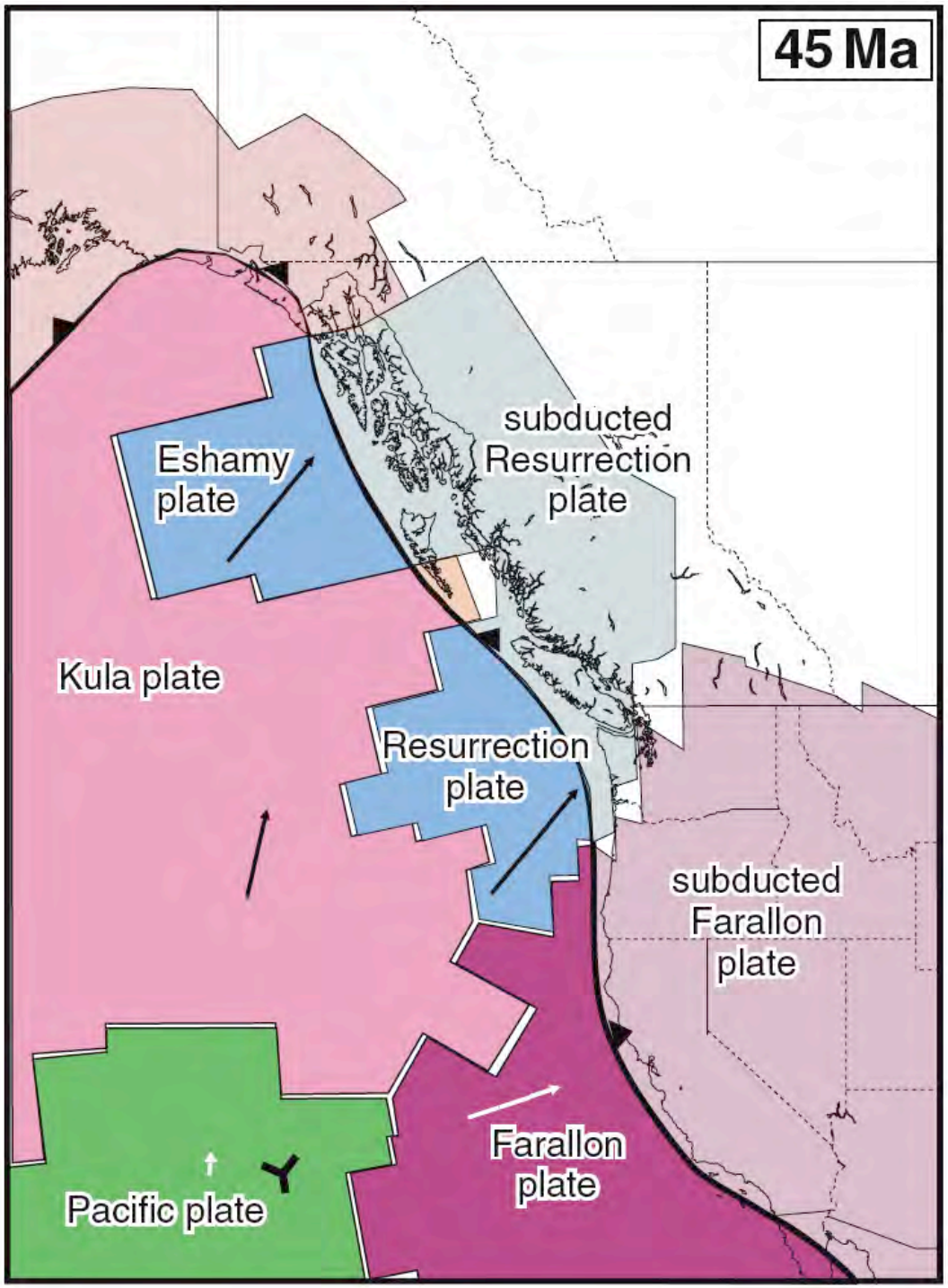

Madsen et al 2006

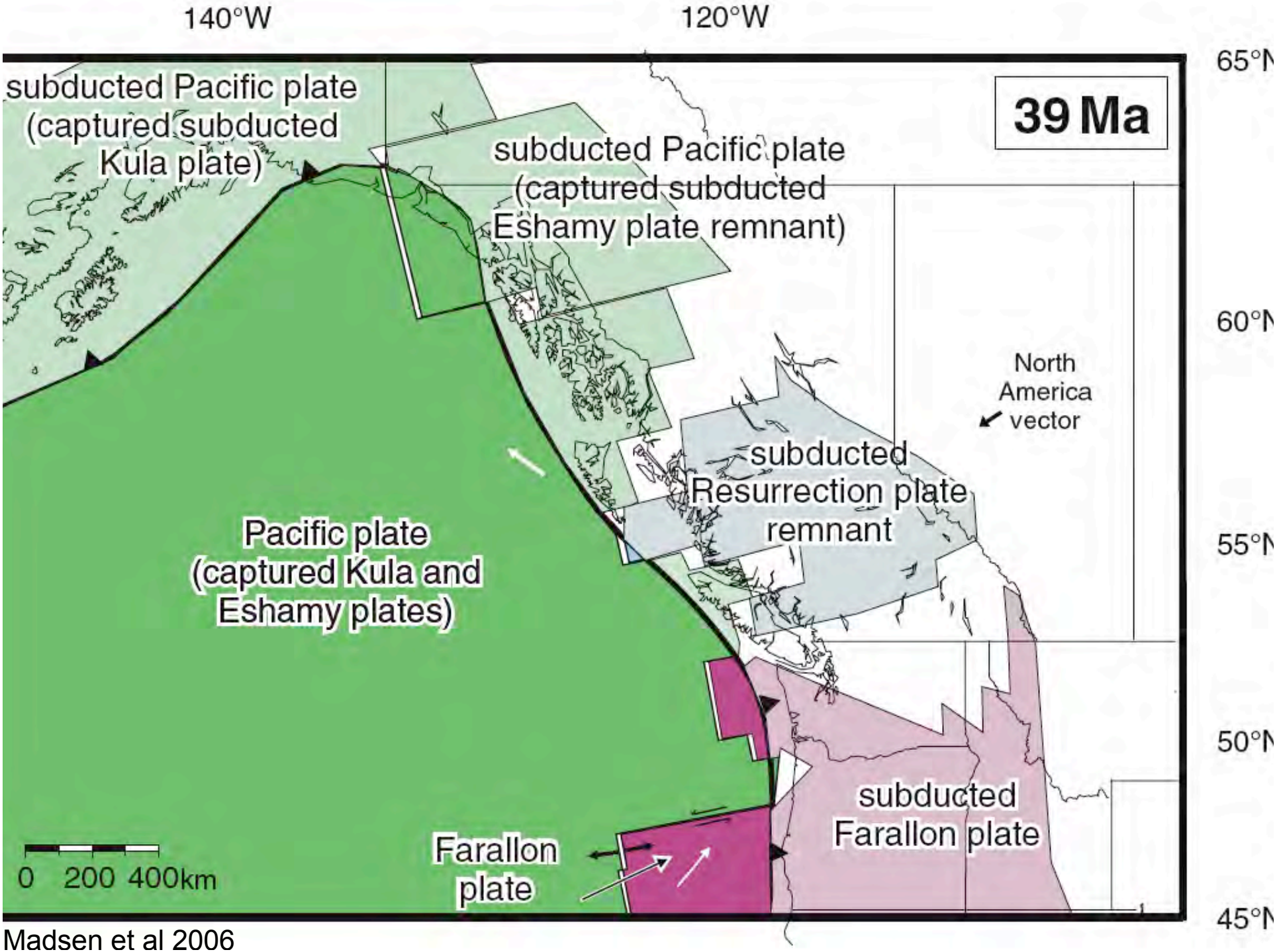

Madsen et al 2006

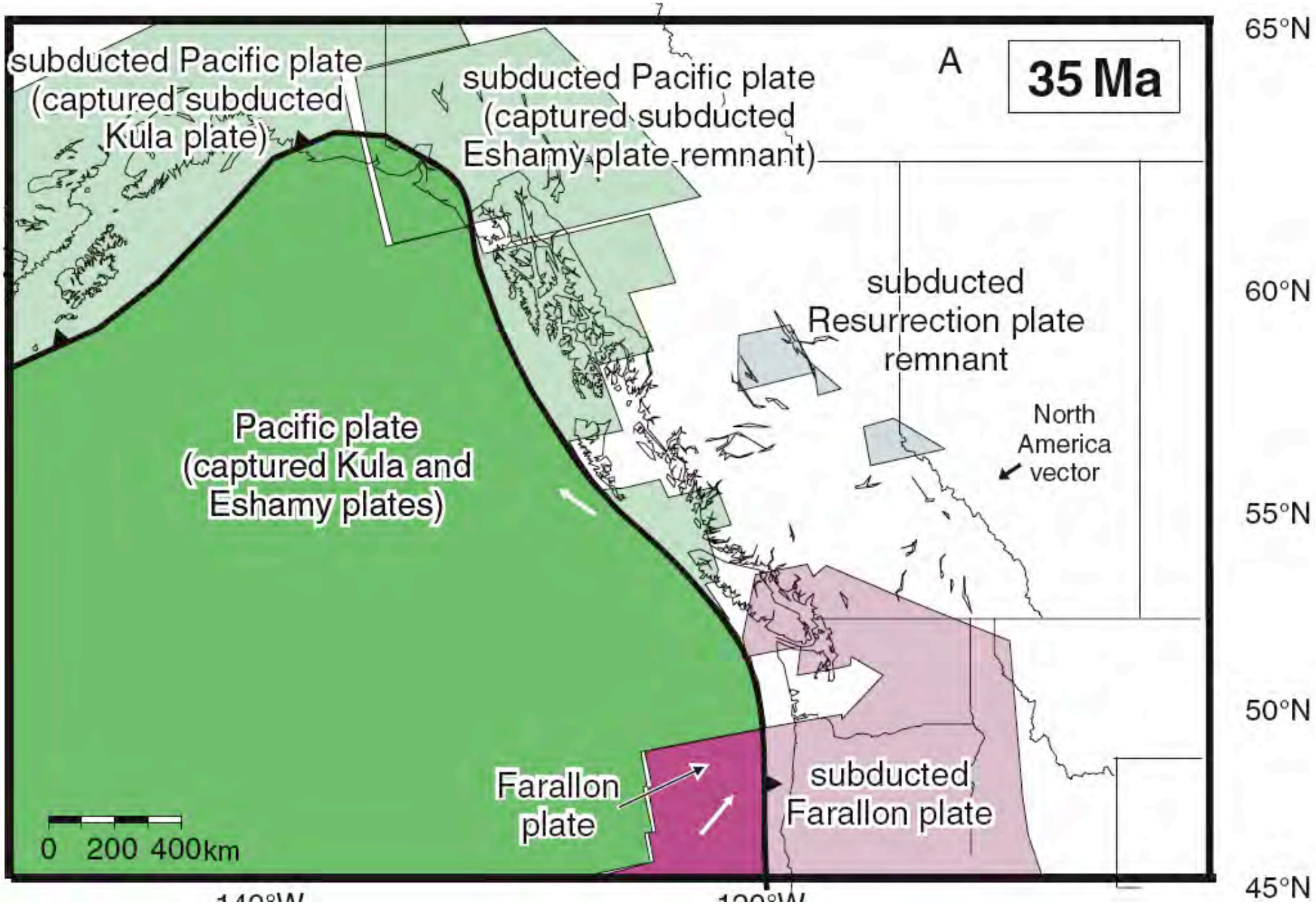

Madsen et al 2006

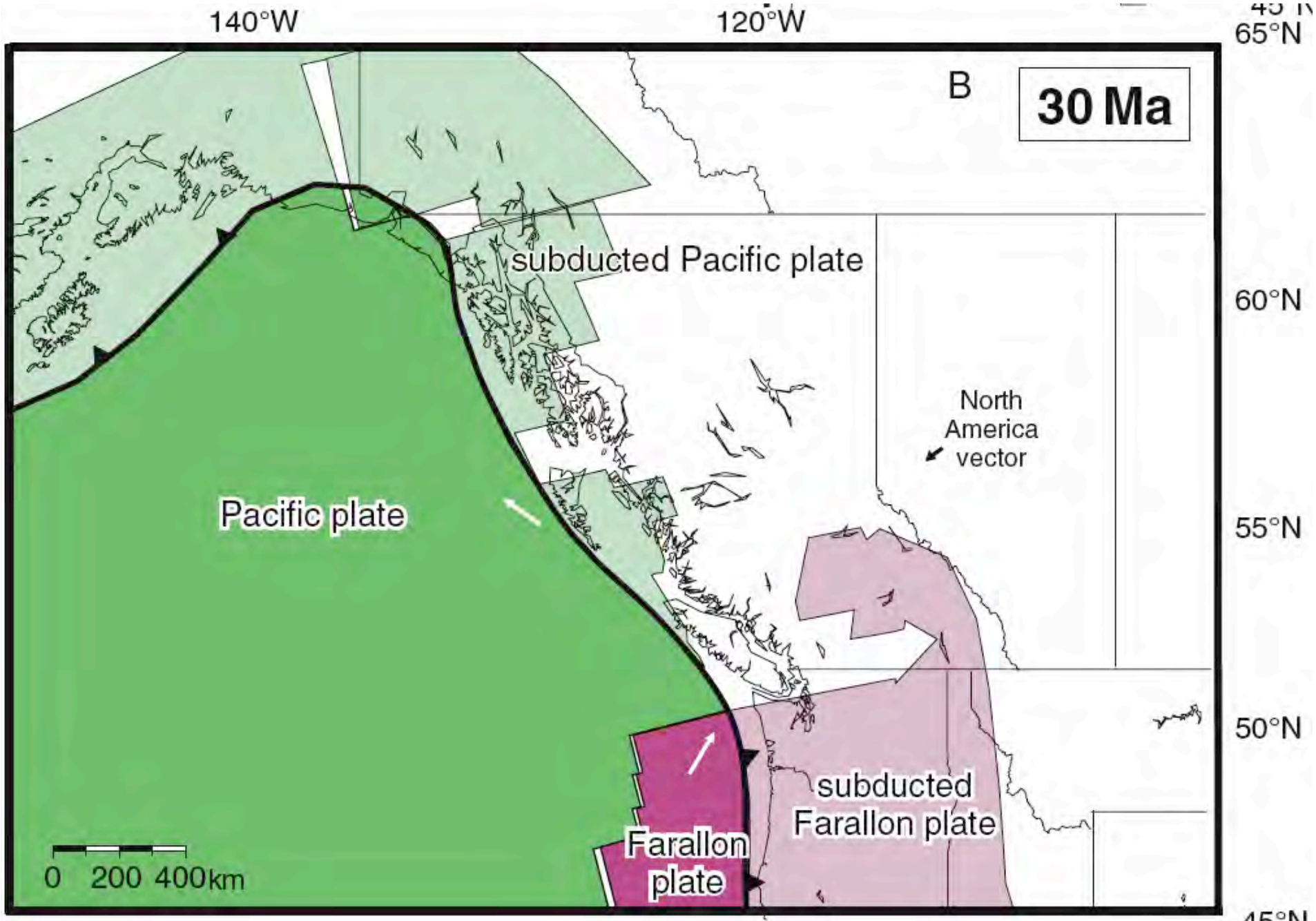

Madsen et al 2006

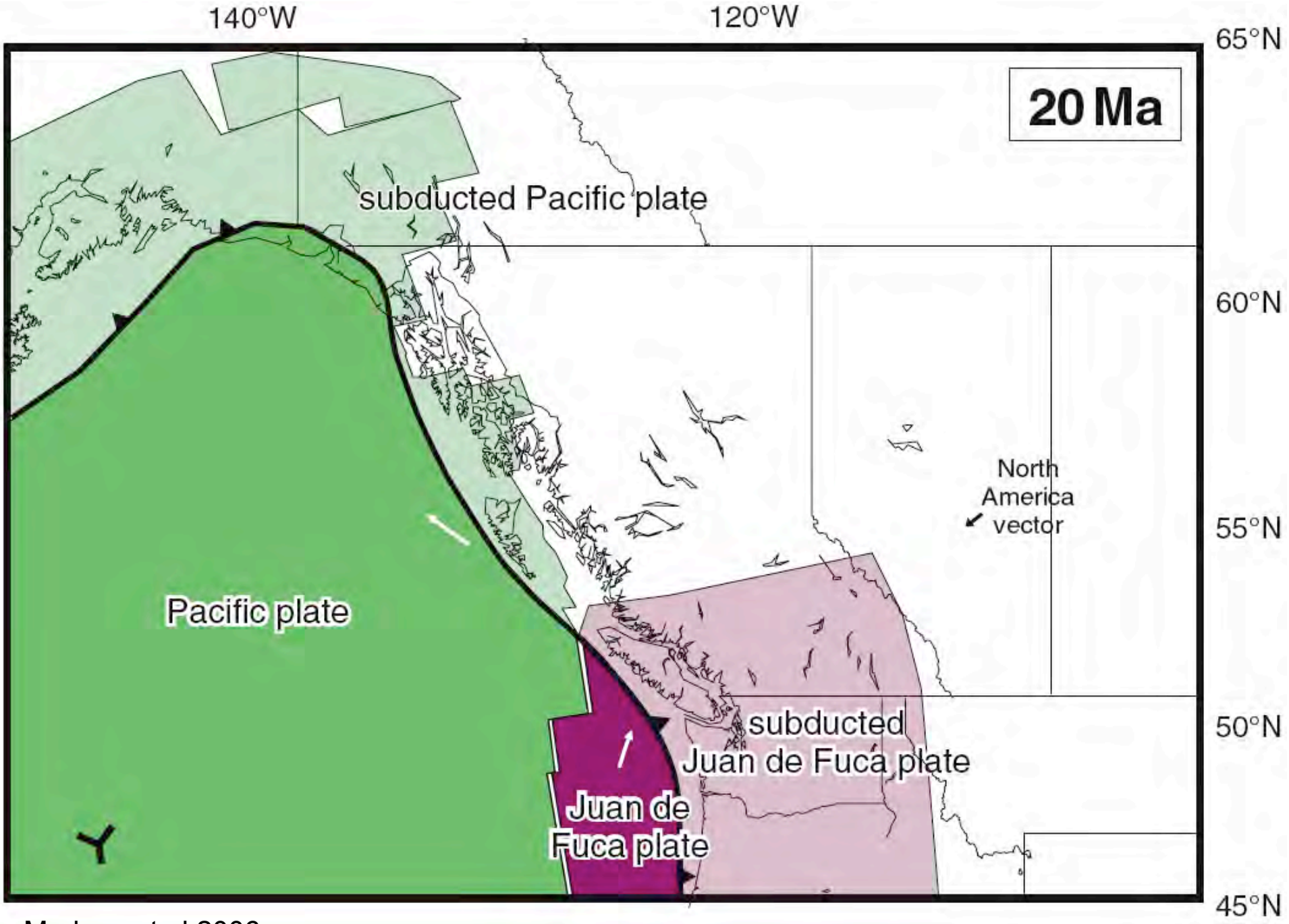

Madsen et al 2006

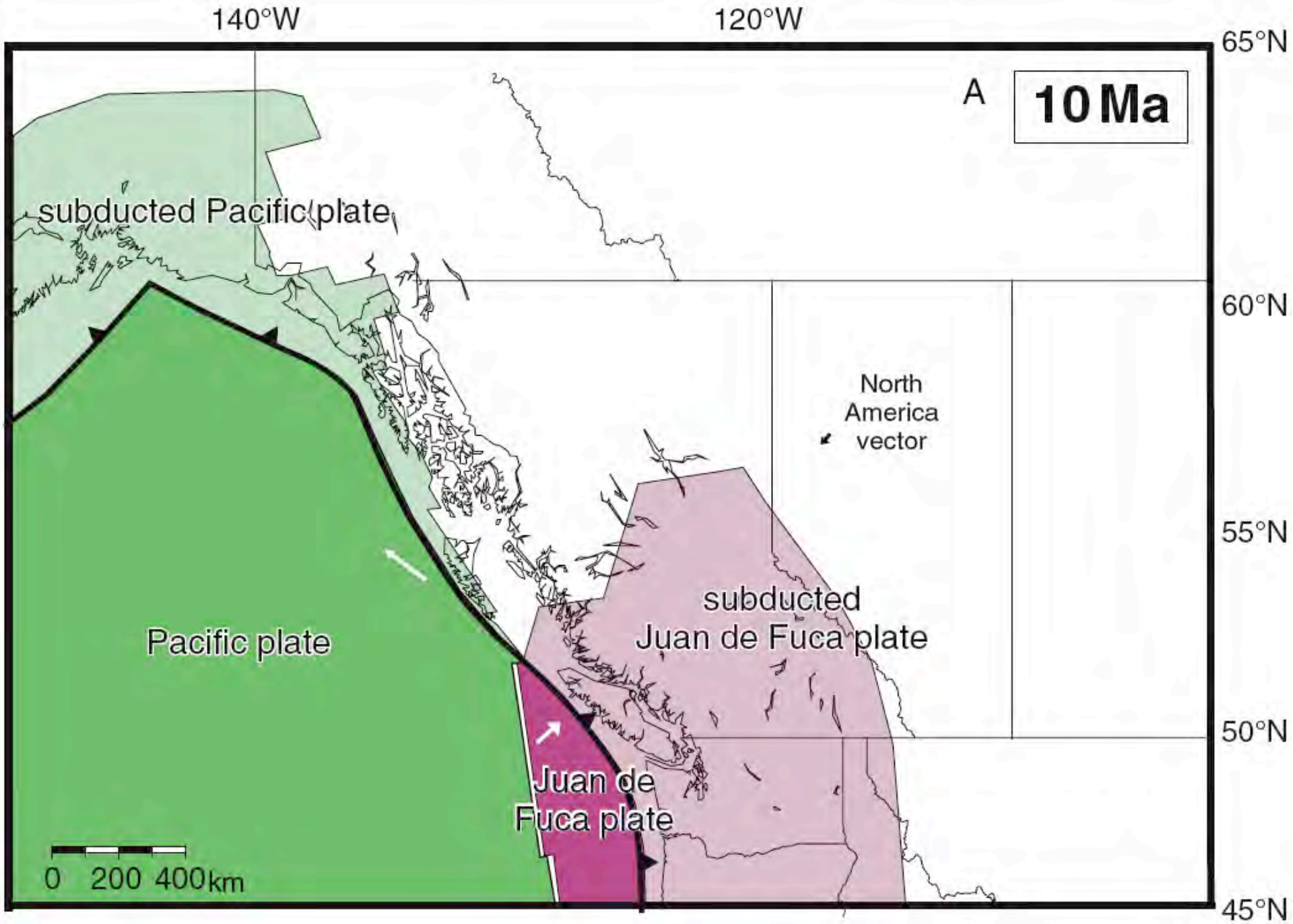

Madsen et al 2006

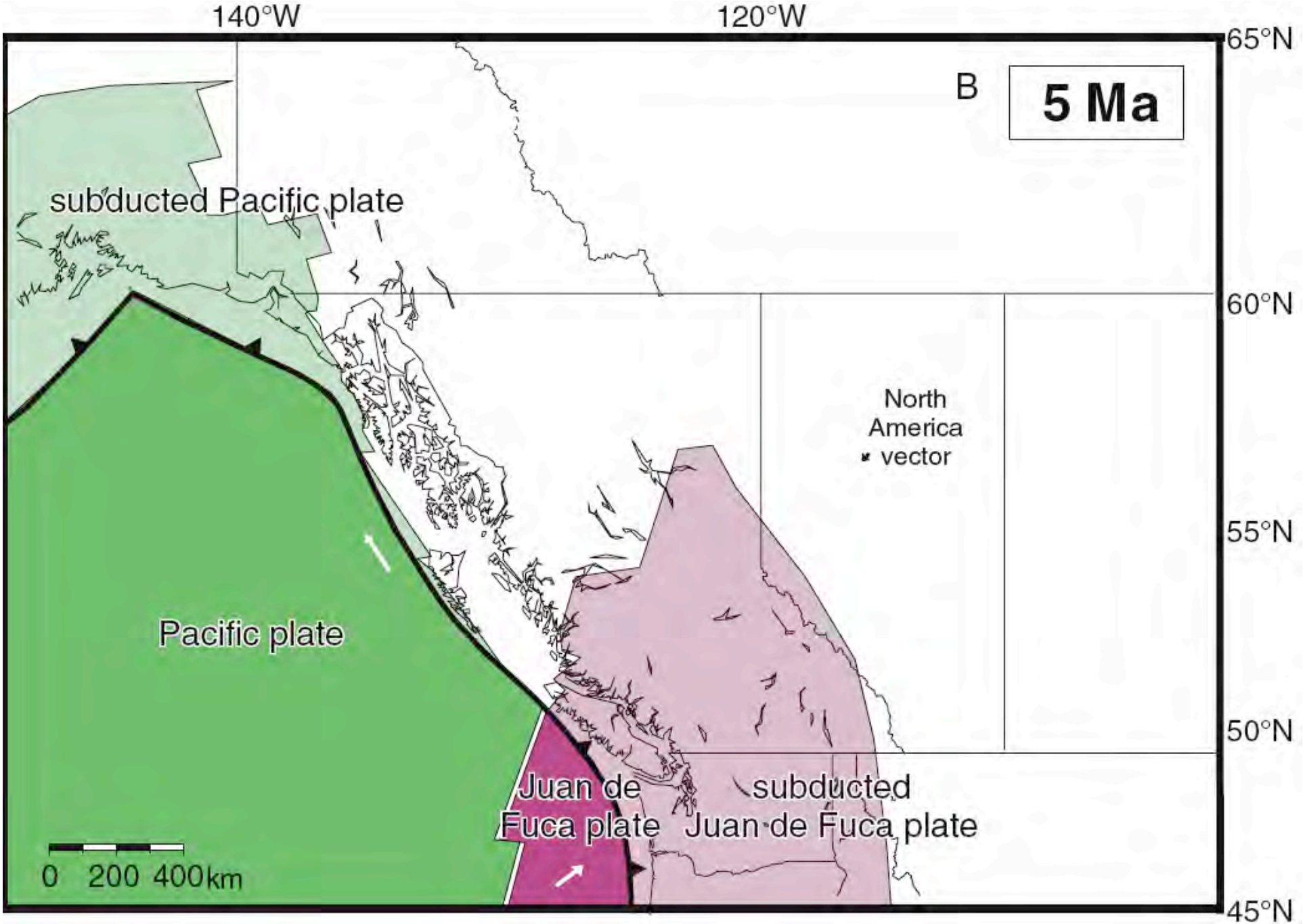

Madsen et al 2006

Madsen et al 2006

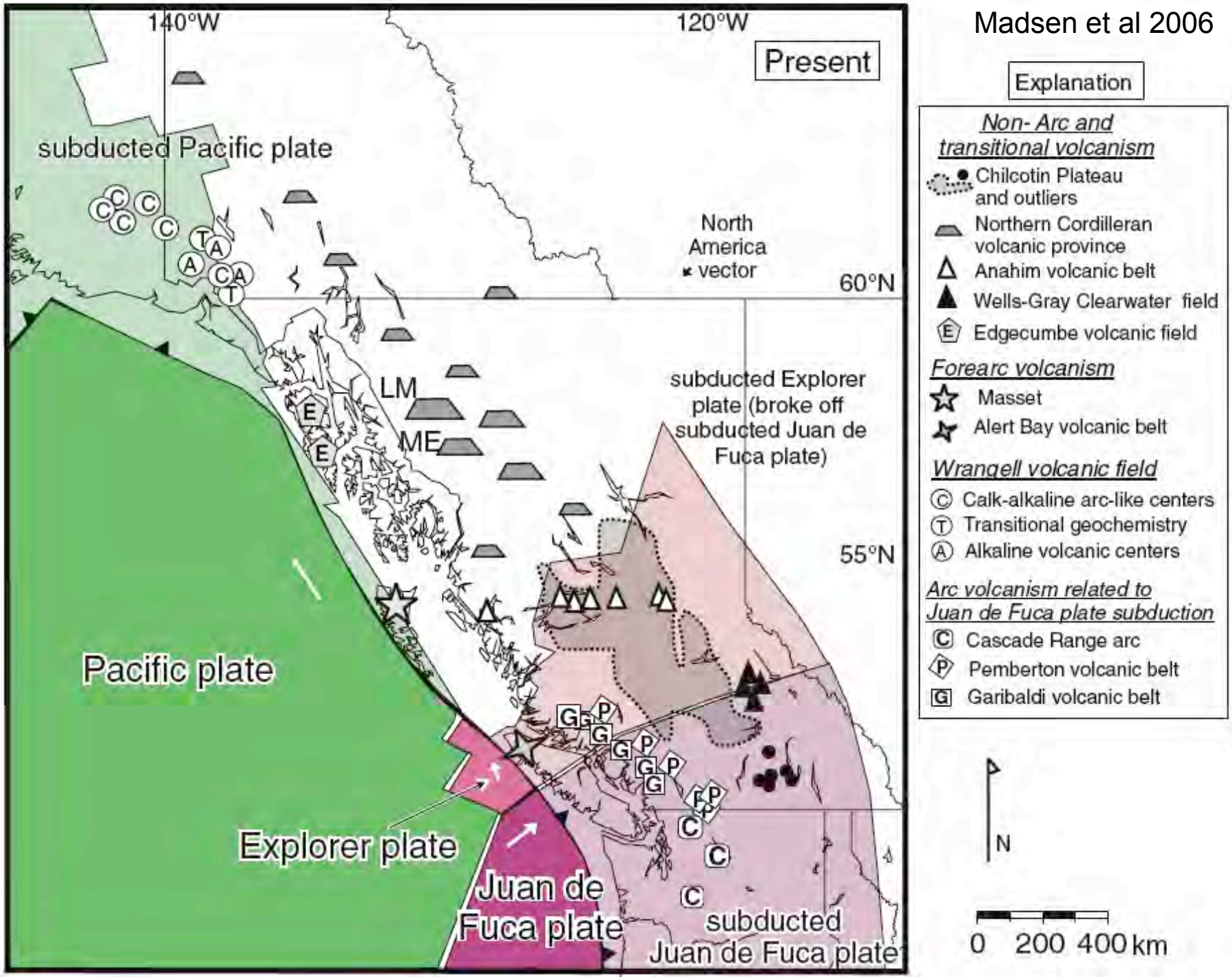

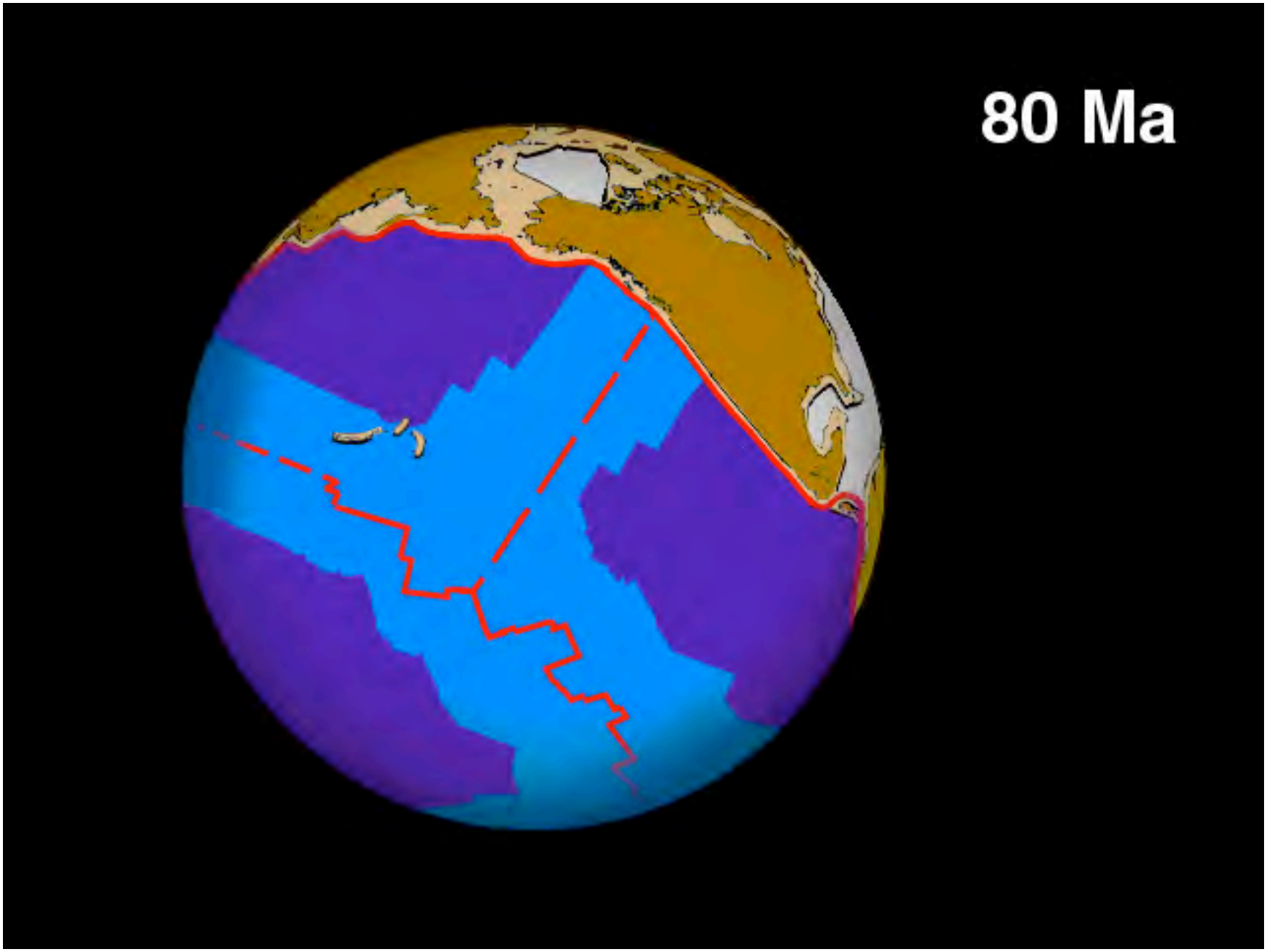
80 Ma